AN ABSTRACT OF THE THESIS OF

ALPHONSE ROMAN NOË for the M. S. in Chemical Engineering
(Name) (Degree) (Major)

Date thesis is presented October 1, 1963

Title LOCAL AND AVERAGE HEAT TRANSFER COEFFICIENTS IN A FLUIDIZED BED HEAT EXCHANGER

Abstract approved Redacted for Privacy
(Major professor)

Local and average heat transfer coefficients for heat transfer from internal tubes to a fluidized bed were investigated. A fluidized bed heat exchanger was compared to a baffled and an unbaffled exchanger in terms of power and heat transfer surface area requirements.

The fluidized bed heat exchanger consisted of a 44 inch long, 5.75 inch inside diameter shell with 19, 3/4 inch diameter tubes arranged in a 1-1/16 inch triangular pitch. Fluidized solids were two narrow sized groups of Scotchlite glass beads having .0057 inch and .0188 inch average diameters. The fluidizing medium was air and there was no tube side fluid.

Variables studied included particle size and concentration, superficial gas velocity, and different locations of the heat transfer surface.

The local heat transfer coefficients were measured by means of a movable temperature probe in contact with the inner wall of a thin-walled tube through which a constant heat flux was maintained.

Values of local coefficients ranging from 2 to 101 Btu/hr. ft^2. °F and average coefficients ranging from 6 to 35 Btu/hr. $ft.^2$ °F were obtained. This represents a maximum increase of 50-fold for the local coefficients and 25-fold for the average coefficients over those for air alone.

The fluidized bed consisted of areas of dense and sparse solids concentration. In the dense section of the bed, the local coefficients were essentially constant and higher values of the coefficients were obtained at lower flow rates. The opposite was true in the sparse section of the bed and variation of heat transfer coefficient with flow rate was similar to that for single phase fluids.

Heat transfer surface location did not affect the average coefficients appreciably, however the local coefficients were affected slightly, the center tube having somewhat lower coefficients.

The average heat transfer coefficients were found to increase as a power function of the solids concentration.

The ratio of the heat transfer capacity of the fluidized bed exchanger to that of the unbaffled and baffled exchangers was considerably greater than unity, indicating its advantage as far as space requirements are concerned.

An overall advantage of reduced heat transfer area and power requirement for the fluidized bed exchanger over the baffled exchanger was found in the region of static bed heights below five inches.

LOCAL AND AVERAGE HEAT TRANSFER COEFFICIENTS IN A FLUIDIZED BED HEAT EXCHANGER

by

ALPHONSE ROMAN NOË

A THESIS

submitted to

OREGON STATE UNIVERSITY

in partial fulfillment of
the requirements for the
degree of

MASTER OF SCIENCE

June 1964

APPROVED:

Redacted for Privacy

Professor of Chemical Engineering

In Charge of Major

Redacted for Privacy

Head of Department of Chemical Engineering

Redacted for Privacy

Dean of Graduate School

Date thesis is presented October 1, 1963

Typed by Jolene Hunter Wuest

ACKNOWLEDGMENTS

The writer takes this opportunity to make the following acknowledgments:

To the Texaco Company for the granting of a fellowship, thereby making this research possible.

To Dr. James G. Knudsen, for his suggestion of the problem and his guidance and encouragement throughout the course of the work.

To Mr. R. C. Mang, scientific instrument technician, for his aid in the design and fabrication of the experimental equipment.

To the Department of Chemical Engineering for the use of its facilities and equipment.

TABLE OF CONTENTS

LIST OF FIGURES

LOCAL AND AVERAGE HEAT TRANSFER COEFFICIENTS IN A FLUIDIZED BED HEAT EXCHANGER

CHAPTER 1

INTRODUCTION

Heat transfer is one of the most important operations in chemical engineering. In industrial practice it is often necessary to transfer heat from one moving fluid to another. The most common form of apparatus for accomplishing this transport of thermal energy is the shell and tube heat exchanger. It consists of a number of tubes arranged parallel to the axis of an outer cylindrical shell. One fluid flows inside the tubes while the other fluid flows outside them. In an exchanger both shell-side and tube-side heat transfer coefficients may be of comparable magnitude in which case both control the capacity of the unit. In some instances one coefficient may be low and it alone is the main controlling factor in the heat transfer rate. If the two streams are of comparable magnitude, the velocity on the shell side is low in comparison with that on the tube side. This is the usual case and for this reason, baffles are installed in the shell to decrease the area of shell-side fluid flow, thereby increasing velocity and turbulence and hence increasing the shell-side heat transfer coefficient (13, p. 500). Such an increase, however, is accompanied by increased pressure losses and hence increased pumping costs. Any means by which velocity and/or turbulence can be increased or by which the boundary layer on the heat transfer surface may be interrupted or reduced in thickness will cause an increase in the heat transfer rate. One means of doing this is to provide a bed of fluidized solid particles on the shell side of the exchanger. Coefficients of heat transfer to fluidized beds are known to be greater than those for single phase fluids alone.

This thesis describes the study of local and average heat transfer coefficients for the transfer of heat from a bundle of internally heated tubes to a surrounding fluidized bed. The test unit consisted of a 5.75 inch diameter shell with 19, 3/4 inch diameter tubes situated in a 1-1/16 inch triangular pitch. The fluidized solid was glass spheres and the fluidizing medium was air in all cases. The local heat transfer coefficient was determined using a movable temperature probe located inside a tubular resistance heating element.

In this study the effects of particle size and concentration, heating tube location, and gas flow rate were investigated. The role of these variables was determined. Hence it was possible to estimate the feasibility of utilizing a fluidized bed for increasing rates of heat transfer in the shell side of a heat exchanger.

This work is exploratory in nature; however, the results obtained indicate that further investigation of fluidized bed heat exchangers is warranted.

CHAPTER 2

THEORY AND LITERATURE REVIEW

Heat may be transferred by any or all of three means; conduction, radiation and convection. Natural convection heat transfer occurs when a temperature difference exists between a surface and the surrounding fluid to which it is exposed. The density of the fluid near the surface is different than that of the main body of fluid giving rise to movement due to buoyant forces. Heat is thus conducted to the fluid and carried away by bulk motion or convection (12, p. 165). Forced convection heat transfer occurs between a surface and a flowing fluid which is pumped along it. Most medium temperature industrial heat transfer is carried out by means of forced convection.

The rate of heat transfer from a solid wall to a fluid flowing past it is proportional to the area of the surface and the temperature difference between the solid and the fluid, i. e.

$$dq_w \propto \Delta T \, dA_w \tag{1}$$

where dq_w is the heat transfer rate from a small element of surface dA_w and ΔT is the temperature difference between the surface and the fluid. Considering a fluid at a bulk temperature, T_b, and a surface whose temperature is T_w, the proportionality becomes

$$dq_w = h \, dA_w \, (T_w - T_b) \tag{2}$$

where h is the proportionality factor and is called the local coefficient of convection heat transfer. Equation 2 may be rearranged to

$$\frac{1}{h} = \frac{T_w - T_b}{dq_w/dA_w} \tag{2a}$$

which is of the form

$$\text{resistance} = \frac{\text{potential difference}}{\text{flux}} .$$

Thus the reciprocal of the heat transfer coefficient becomes equivalent to a resistance to heat transfer.

In the turbulent flow of a fluid past a solid boundary, three flow zones exist: (1) a thin laminar sublayer at the wall, (2) a turbulent core occupying most of the cross section of the stream and a (3) a buffer zone between them. The major resistance to heat transfer between solid boundaries and turbulent fluids is the laminar sublayer adjacent to the wall. The heat must flow through the laminar layer by conduction, i. e.

$$q = \frac{k\ A\ \Delta T}{x} \tag{3}$$

where k is the fluid thermal condutivity, Btu/hr ft.^{2} °F/Ft

A = area normal to heat flow, ft.^{2}
q = heat flow, Btu/hr.
ΔT = temperature difference, °F
x = thickness of the boundary layer, ft.

It is seen that the resistance of this layer is proportional to its thickness and any reduction of the thickness will result in a comparable increase in the rate of heat transfer between the wall and the fluid. One means of reducing the thickness of the laminar layer is by increasing the intensity and scale of the turbulence of the main flowing stream.

Studies of the effect of turbulence promoters on the rate of heat transfer have been made (9, p. 396) and it has been shown that the rate of heat transfer is materially increased. Also, baffled heat exchangers which force the shell side fluid to flow through a decreased cross section and normal to tube banks, thereby increasing turbulence, have greater heat transfer capacity than unbaffled exchangers. For example the correlation of shell side heat transfer coefficients as proposed by Donohue (3, p. 2501) illustrates the larger magnitude of heat transfer in the baffled exchanger over that in the unbaffled case; For unbaffled heat exchangers

$$\frac{h_{av.}\, d_o}{k} = 0.128\, d_e^{0.6} \left(\frac{d_o\, G}{\mu}\right)^{0.6} \left(P_r\right)^{1/3} \left(\frac{\mu_b}{\mu_w}\right)^{0.14} \qquad (4)$$

where d_e is the equivalent diameter in inches based on four times the hydraulic radius; For segmental baffles

$$\frac{h_{av.}\, d_o}{k} = 0.25 \left(\frac{d_o\, G_e}{\mu}\right)^{0.6} \left(Pr\right)^{1/3} \left(\frac{\mu_b}{\mu_w}\right)^{0.14} . \qquad (5)$$

A comparison of these equations indicates a higher coefficient in the baffled exchanger. The intensity of turbulence around a surface, such as a tube wall, may also be increased by the addition of fluidized solid particles to the shell side fluid. Thus the heat transfer attributes of a fluidized bed may be helpful when considering heat exchanger design, especially where compact exchangers are desired.

Fluidized Bed Heat Transfer

A great deal of research on fluidized bed systems has been done in recent years. One of the outstanding characteristics of a fluidized bed is that it tends to maintain a uniform temperature even with non-uniform heat release. Close temperature control is possible since the solid particles in a fluidized bed act as reservoirs and carriers of heat. Their violently turbulent motion enables them to absorb heat in various parts of the system thus eliminating hot and cold spots. This makes fluidized beds particularly useful for carrying out chemical syntheses which require limited temperature ranges. The majority of research on the heat transfer characteristics of fluidized beds has been performed with this in mind. Little consideration has been given to the applicability of fluidized beds to increasing heat exchanger capacities (6).

Fluidized bed heat transfer may be divided into three sections:

(1) Fluid to particle heat transfer

(2) Heat transfer between points within the bed

(3) Bed to surface heat transfer

The rate of fluid to particle heat transfer is used to estimate particle surface temperature from the measured temperature of the fluid. This is useful in predicting heat effects on heat sensitive particles. Frantz (5), Gupta and Thodos (8), and Yeh (22) have presented correlations for determining fluid-to-particle heat transfer coefficients.

Heat transfer between points within a bed occurs at a high rate due to the rapid mixing, and hence does not affect design greatly. Investigations have shown that the fluidizing gas rapidly reaches the temperature of the bed (5). Yagi, Kunii and Wakao have given a correlation (21) for effective radial thermal conductivities. Bischoff (2) presented a method for obtaining values of axial thermal conductivity. Gopalarathaam, Hoelscher and Ladda (7) have extended the method of Kunii et. al. to liquids. Lewis, Gilliland and Girouard (11) found that effective thermal conductivities in the radial direction were about 2 percent of that in the longitudinal direction.

Much attention in the technical literature is directed to bed-to-surface heat transfer since it is often necessary, in an industrial operation, to remove or add heat to a fluidized system.

Coefficients of heat transfer to fluidized beds are known to be higher than those to single phase gases alone. Coefficients to gases are normally about 0.5 to 5 Btu/hr. ft.^{2} °F at the gas velocities used in fluidized beds, while coefficients to fluidized beds usually range from 20 to 100 Btu/hr. ft^2 °F (6). Considerable work has been done to determine heat transfer coefficients to fluidized beds and generalized correlations have been given. Of the attempts at a generalized correlation for fluidized bed-to-wall heat transfer coefficients those of Wen and Leva (19) and Wender and Cooper (20) are recommended.

Wen and Leva correlated the data of four investigations using conventional techniques. The data covered a broad range of test materials including glass beads and materials such as coke, iron powder, lead, etc.

Richardson and Smith (16) studied improvements in heat transfer coefficients caused by the presence of particles over that obtained with liquid at the same velocity and correlated this in terms of the properties and concentrations of the particles and the liquid velocity. They studied particles, approximately spherical, of Ballotini glass, gravel, iron, copper and lead.

Mickley and Trilling (14) obtained data on internally and externally heated fluidized beds and presented a correlation for various glass bead sizes.

Vreedenburg (18) (17) presented correlations for heat transfer between fluidized beds and vertical and horizontal tubes. He also gives a correction factor for non-axial location.

Wender and Cooper (20) gave a correlation for axial vertical tubes:

$$\frac{h D_p}{k(1-\epsilon)} \left(\frac{k}{C_g \rho_s}\right)^{0.43} = 0.033\, C_r \left(\frac{D_p G}{\mu}\right)^{0.23} \left(\frac{C_s}{C_g}\right)^{0.80} \left(\frac{\rho_s}{\rho_g}\right)^{0.66}$$

C_r is the correction factor for non-axial tube location proposed by Vreedenburg. The correction factor ranges from 1.0 at the axial position to a maximum 1.8 at approximately 30 percent of the radial distance from the vessel center line, decreasing thereafter.

All correlations are based on data obtained with clean equipment and are valid for single tubes only.

CHAPTER 3

EXPERIMENTAL EQUIPMENT

The experimental apparatus was designed in order to determine the local and average heat transfer coefficients from an internal heat source to a fluidized bed.

It consisted of an internally heated fluidized bed unit, an air source, a direct current source and associated metering and measuring devices. A schematic drawing of the apparatus is presented in Figure 1. The actual equipment set up is shown in Figure 2. The major components are described in detail below.

Fluidized Bed Unit

The fluidized bed unit consisted of a tube bundle containing a heating element and a shell. The shell consisted of a conical air distributing section, a test section and a disengaging section.

The sheet metal conical air intake was 5.75 inches in diameter by two inches in diameter and the overall length was six inches. A sheet metal extension of two inch diameter and three inch length was spotwelded to the cone.

The disengaging section, to prevent elutriation of glass beads, was a nine inch OD by 1/8 inch wall, 12 inches long, cast acrylic tube, Six, 1.5 inch diameter exhaust ports were cut into the tube

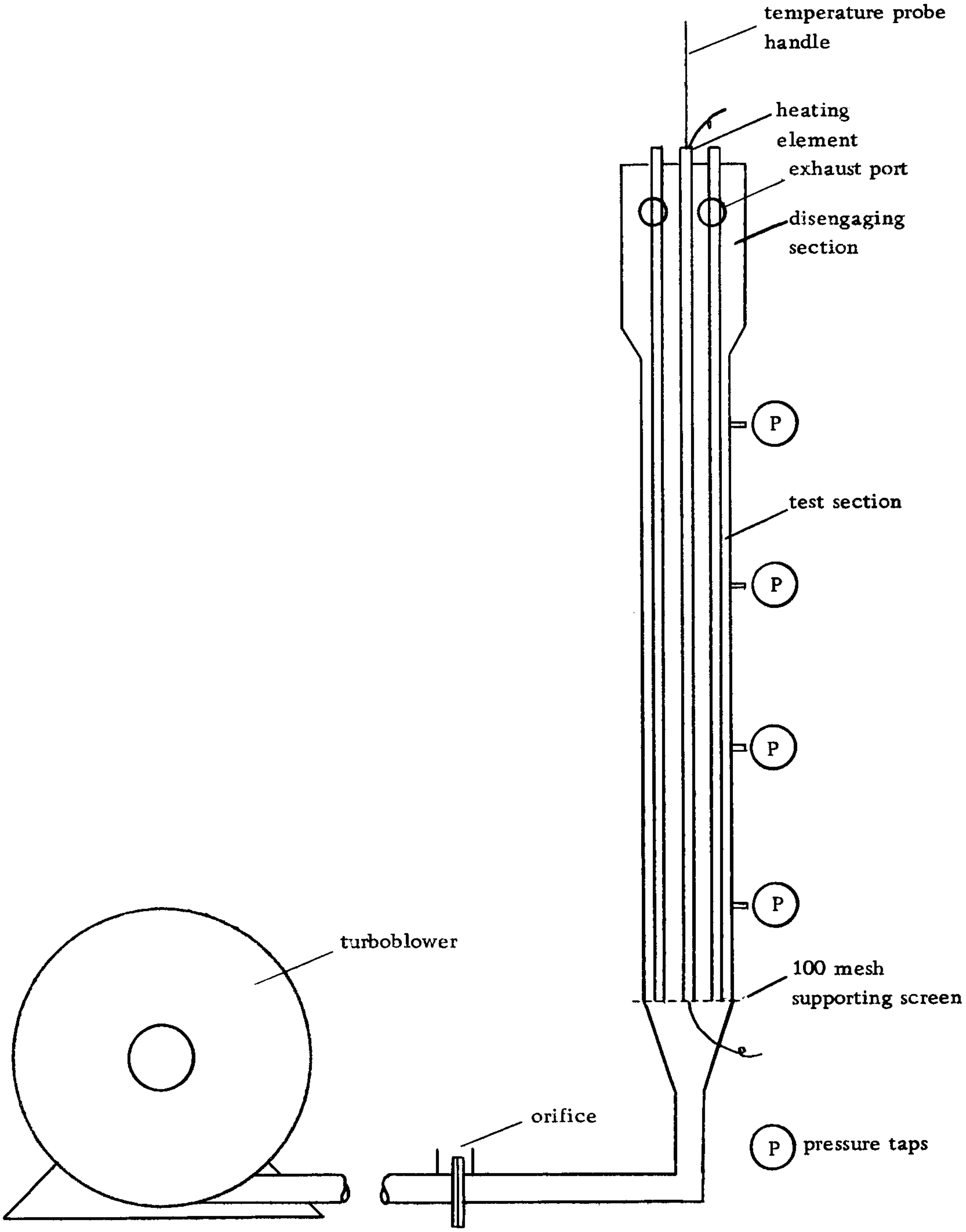

Figure 1. Diagram of Apparatus

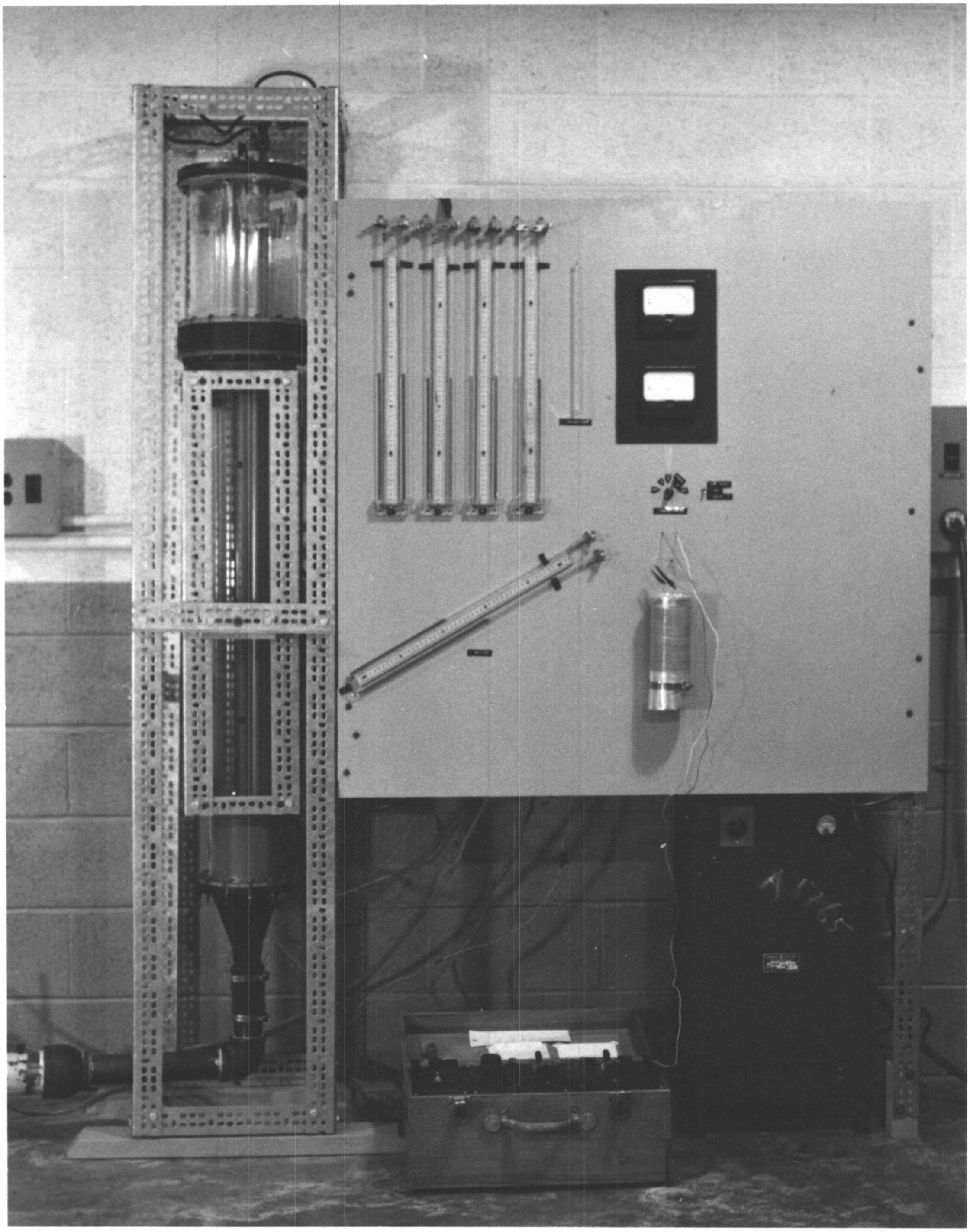

Figure 2. Fluidized Bed Unit

2.5 inches from the top and covered with 100 mesh wire cloth. To connect the disengaging and test sections, a conical enlarging section fabricated from two, one inch thick plywood disks of 11 inch diameter was provided. The test unit, connecting section and disengaging section were joined by flanges cut from 1/2 inch plexiglass sheet and glued to the acrylic tubes. Sixteen 3-1/2 by 1/4 inch bolts secured the flanges.

The test section was constructed from a six inch OD by 1/8 inch wall, 44 inches long, cast acrylic tube. Four pressure taps located 5-1/2 inches from the bottom of the tube and every 11 inches thereafter were affixed to the test section. The taps, fabricated from a one inch length of 3/4 inch diameter plexiglass rod shaped to a 1/4 inch diameter by 3/4 inch deep connection, were glued to the test section, drilled with a 1/16 inch drill and 100 mesh wire cloth placed over the outside openings. The test section was attached to the air intake section with a 1/2 inch thick, seven inch diameter, plastic flange and secured by 12, 2 by 1/4 inch bolts.

The tube bundle consisted of 18, 3/4 inch OD, 60 inches long aluminum condenser tubes and one, 3/4 inch OD stainless steel heating element arranged in a 1-1/16 inch triangular pitch. The tube layout is shown in Figure 3. One end of each tube was fitted with a 3/4 inch plastic plug to facilitate fitting into the lower tube sheet.

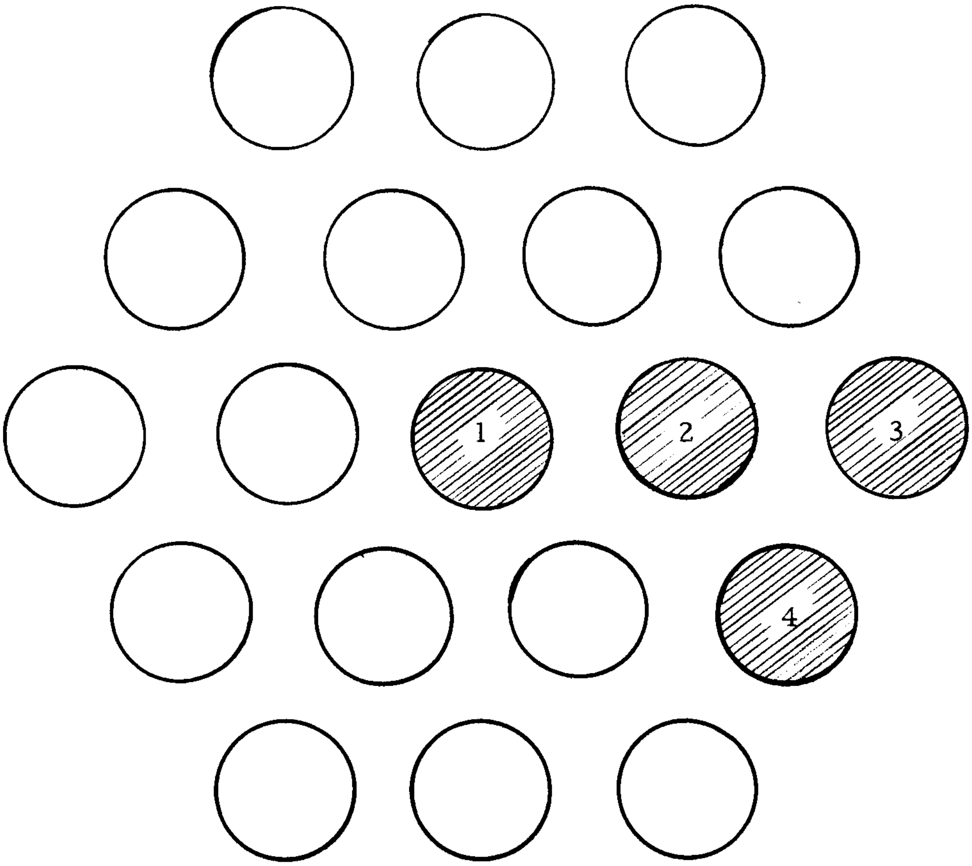

Figure 3. Tube Layout: Showing Locations of Heating Element

The top tube sheet, fabricated from two, one inch thick plywood disks of 11 inch diameter, was connected to the disengaging section by six, 2 by 1/4 inch bolts.

The bottom tube sheet, placed between the air intake and test sections, consisted of 100 mesh wire cloth placed on 14 mesh wire screen. Three-eighths inch diameter holes with the edges soldered to prevent unraveling were punched into it.

The heating element, type 321 stainless steel with a resistivity of 72×10^{-6} ohm-cm., had a 3/4 inch OD by .012 inch wall by 60 inch length. The bottom of the tube was fitted with a 3/8 inch diameter plug with a 1/4 inch hole to accept number six copper wire; a set screw held the wire. The top of the tube was fitted with a three inch long copper plug with a 5/16 hole and 1/32 inch plastic bushing to facilitate sliding of the probe handle. The copper lead wire was attached with a solderless connector.

The entire unit excluding the air intake was mounted in a three feet long "cradle" of 2-1/4 by 1-1/2 inch slotted angle iron. This was mounted inside a 7-1/2 feet high vertical frame so as to permit the unit to be positioned vertically for operation and horizontally for tube removal.

Air Source

Air was supplied from a turboblower manufactured by The North American Manufacturing Company, Cleveland, Ohio. The blower had a rated capacity of 100 cubic feet per minute at 16 ounces per square inch discharge pressure. The blower was powered by a three phase, 220 volt, one and a half horsepower induction motor manufactured by the General Electric Company, Schenectady, New York. The air flow was controlled by means of a slide valve located on the intake of the blower. Three inch N. P. S. standard steel pipe was used to carry the air to the fluidized bed unit and connected by means of a reducer to a two inch N. P. S. pipe and by rubber hose to the air intake section.

The air was metered by means of a two inch diameter, 16 gauge square edged orifice located in the three inch pipe. The orifice was machined accurately and precisely from smooth brass plate to desired specifications and radius taps located at the proper distance so that the expansion factor and coefficient of discharge could be calculated by accepted methods.

Power Source

Direct current to heat the stainless steel tube was supplied from a copper oxide battery charger manufactured by the General Electric Company, Schenectady, New York. The battery charger had a direct current output rating of 12 volts and 45 amps. A constant voltage transformer manufactured by the Sola Electric Company, Elk Grove, Illinois was placed in the line to insure constant current output.

A schematic diagram of the electrical system is presented in Figure 4. Seven, four ohm 200 watt vitreous enameled variable resistors manufactured by the Ohmite Manufacturing Company, Skokie, Illinois were also used in the system. These resistors were set at three ohms each and placed in parallel to draw a current of approximately 36-38 amps. This resistance was placed in series with the heating element.

The emf and current were measured by a D. C. voltmeter with a range of 0-3 volts and a D. C. ammeter with a range of 0-50 amps. Both instruments were manufactured by Simpson Electric Company, Chicago, Illinois. Number six plastic insulated copper wire and solderless connectors completed the circuit.

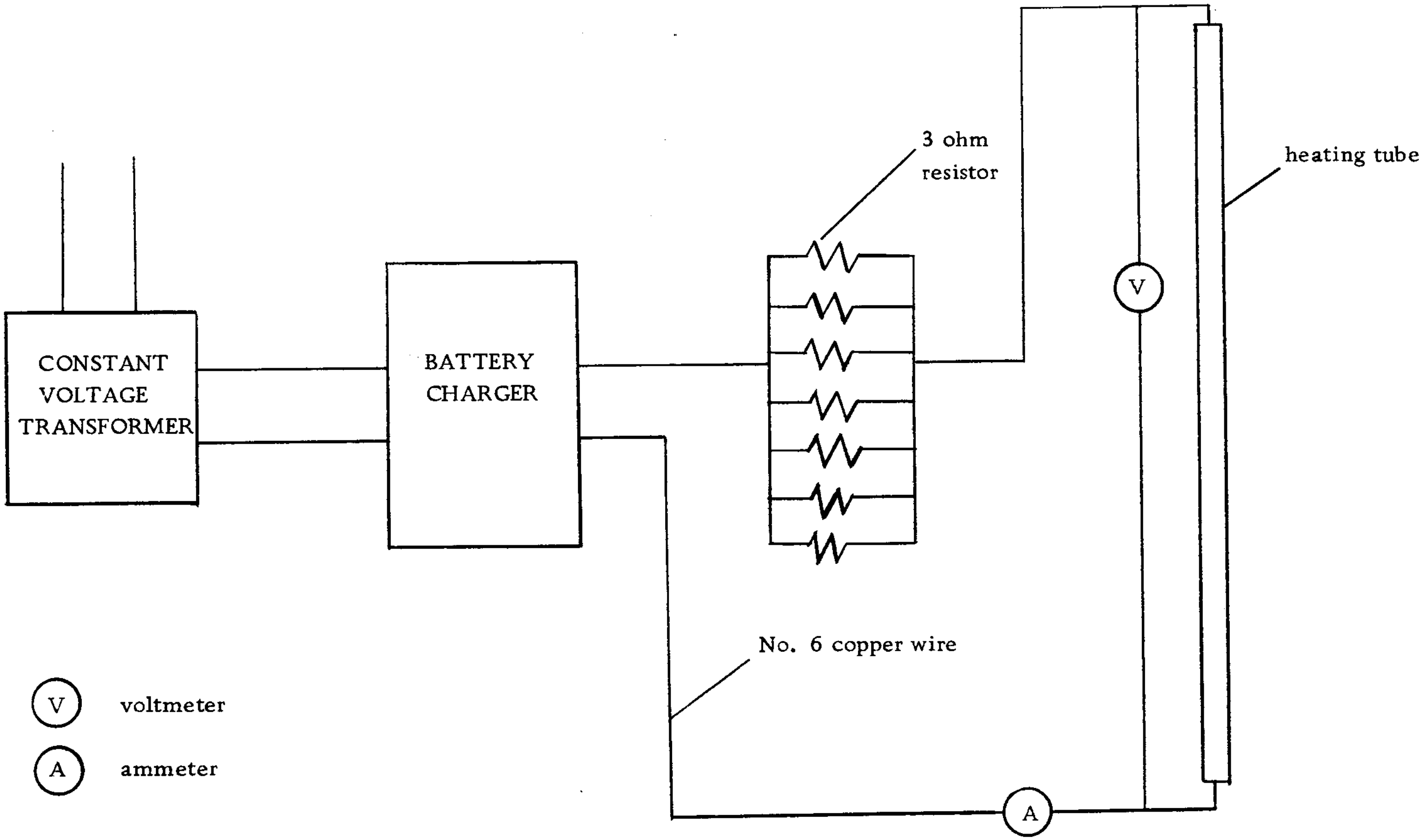

Figure 4. Diagram of Electrical System

Measuring Devices

The pressure drop across the bed and orifice was measured by a manometer system using water as the manometer fluid.

The wall temperature of the heating element was measured at various positions, without affecting fluid flow, by designing a thermocouple probe which moved up and down inside the heating element. An exploded view of the probe is shown in Figure 5. The main body of the probe was fabricated from micarta plastic. The wall contacts consisted of two, 1/8 by 3/16 inch diameter pieces of copper rounded to form a flush contact with the heating tube wall. A hole 1/16 inch in diameter by 1/16 inch deep was drilled into each copper contact. Two 1/64 inch holes were drilled in each of two micarta disks 1/16 inch diameter by 1/16 inch thick. A groove 3/128 inch deep was cut between the holes. Thermocouple wire was threaded through each of these disks and the thermocouples formed. The thermocouple junctions were placed in the grooves and the disks inserted into the copper contacts and sealed with epoxy glue. The thermocouple junction does not contact the copper so as to prevent electrical effects from the heating element affecting the probe reading. The copper contacts were then fitted with a small wire spring and inserted into the two, 3/16 inch holes in the main body. The thermocouple leads were brought

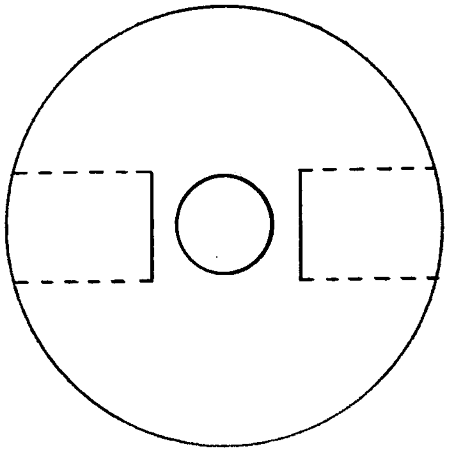

Top View

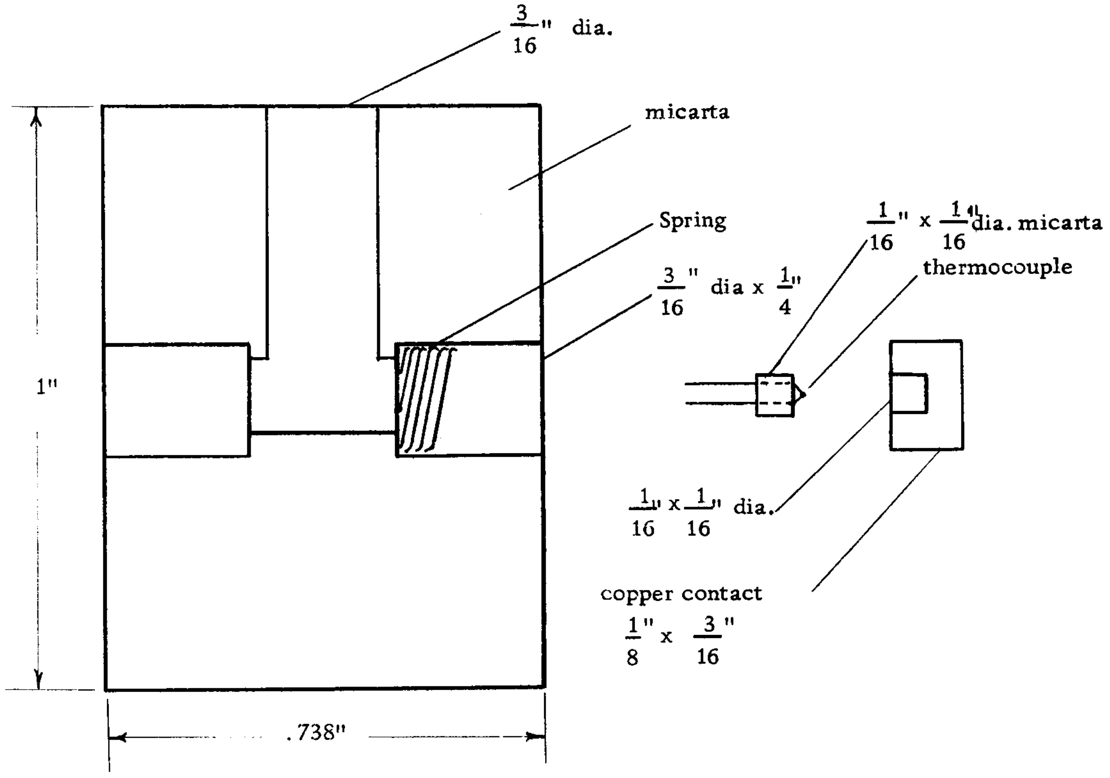

Front View

Figure 5. Exploded View of Temperature Probe

out through the 1/8 inch hole drilled into the center of the probe body. This hole was tapped to a width of 5/16 inch and a depth of 1/2 inch and a five and one half foot by 1/4 inch hollow aluminum rod fastened to the probe with a 5/16 inch tube fitting. The thermocouple leads were brought up through the center of the rod. The probe was fitted inside the heating element and both used as one unit.

All temperatures were measured using iron-constantan thermocouples formed by fusing the ends in an acetylene flame. The wire used was number 30 B. and S. Gauge, single-cotton-covered and enameled, Leeds and Northrup thermocouple wire. Thermocouple emf was read using a Leeds and Northrup potentiometer number 674933.

The probe thermocouples were connected in series to read twice the average probe temperature as were the two thermocouples located in the air intake section. A single thermocouple was placed in an oil bath in a 12 inch long copper tube and inserted in the disengaging section of the unit. All reference junctions were kept in an ice bath at 32 degrees Fahrenheit.

By means of a suitable switching system it was possible to read directly, in emf, twice the probe temperature, twice the air inlet temperature, the air outlet temperature and twice the temperature difference between the probe and air inlet. A Leeds and

Northrup type G Speedomax recorder was used to record the probe temperature and thus indicate when steady state had been reached.

CHAPTER 4

EXPERIMENTAL PROGRAM

The purpose of this investigation was to determine the local and average heat transfer coefficients for heat transfer from a heated tube to a fluidized bed.

There are many factors which may affect the transfer of heat from an internal source to a fluidized bed. These may be classified under three general headings; (1) properties of the materials, (2) operating conditions and (3) equipment design.

Under material properties one may consider thermal conductivity, density and viscosity of the fluidizing medium and of the fluidized solid. Operating conditions include size, distribution and shape of particles, solid concentration, gas velocity, heat flux and the magnitude of temperature driving forces. Heat transfer surface location and size, and fluid bed geometry are variables of equipment design.

The variables studied in this investigation included particle size and concentration, superficial gas velocity, and location of the heat transfer surface. Air was used as the fluidizing medium and only one tube bundle was studied.

Particle Size

The solid particles employed were Scotchlite glass beads manufactured by the Minnesota Mining and Manufacturing Company. Two size groups having average diameters of .0188 inch and .0057 inch and numbered 070 and 110 respectively by the manufacturer were used. These shall be referred to as coarse and fine beads. The density of glass beads is 156 $lbs/ft.^3$ In order to have as narrow a size range as possible, the glass beads were screened to give 20/35 mesh and 65/100 mesh ranges. The size distribution of the beads is shown in Figure 6. Average particle diameter was determined by taking the arithmetic average of measurements of photo-micrographs of the beads. These are presented in Figure 7. It can be seen that the fine beads are generally spherical and similar in size while there are considerable irregularities among the coarse beads.

Particle Concentration

Particle concentration in the bed varied from zero to approximately 55 lbs/ft^3. The concentration was regulated by charging various known amounts of beads into the unit. The amount was measured as static bed height by a scale affixed to the test unit shell. The charge was fluidized and allowed to settle twice and make-up added to the desired mark so as to assure the same degree of packing for

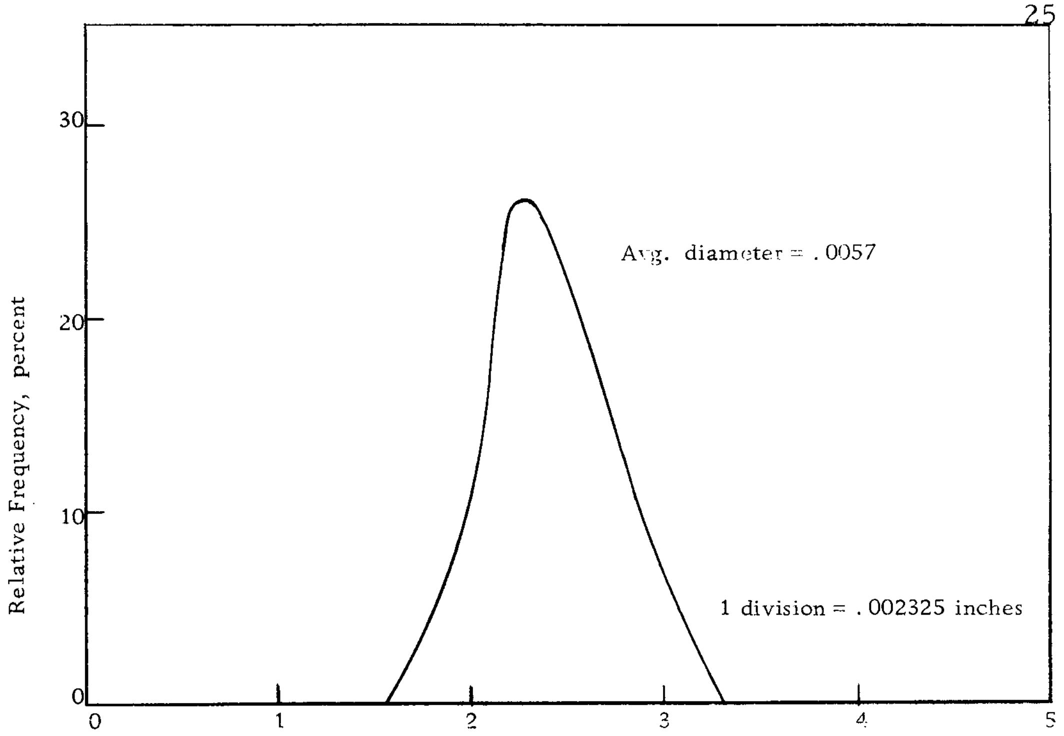

Scotchlite Glass Beads No. 110

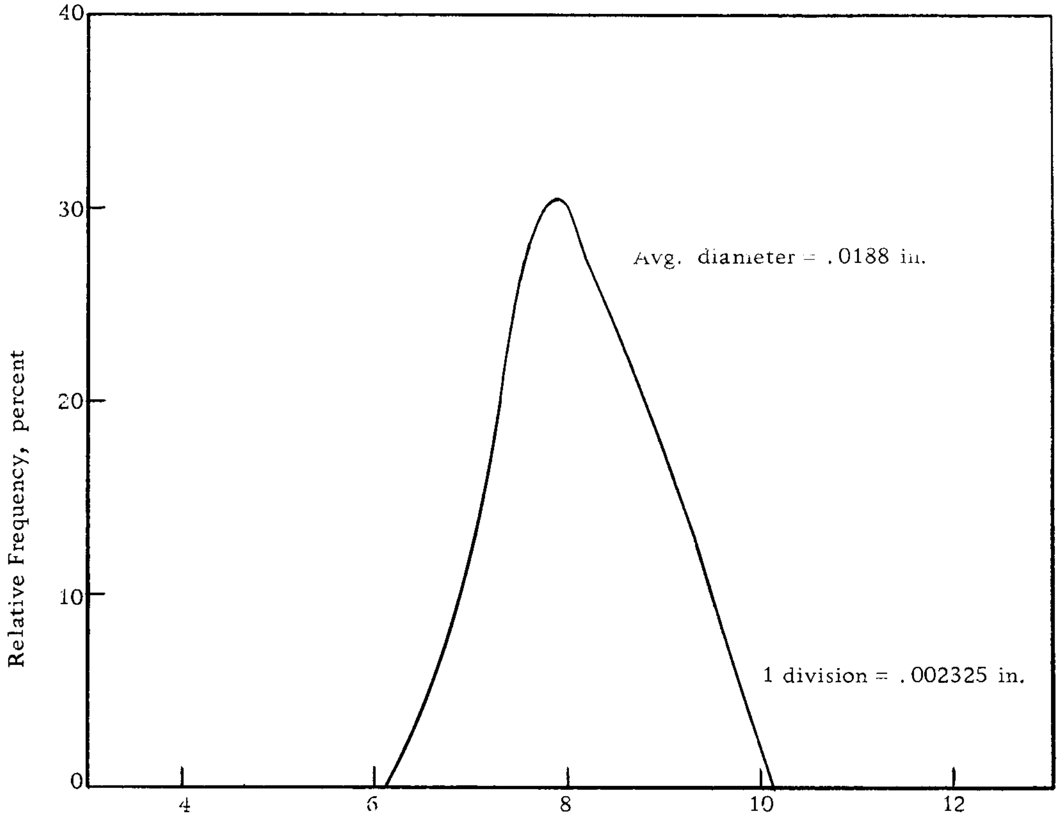

Scotchlite Glass Beads No. 070

Figure 6. Glass Bead Size Distribution

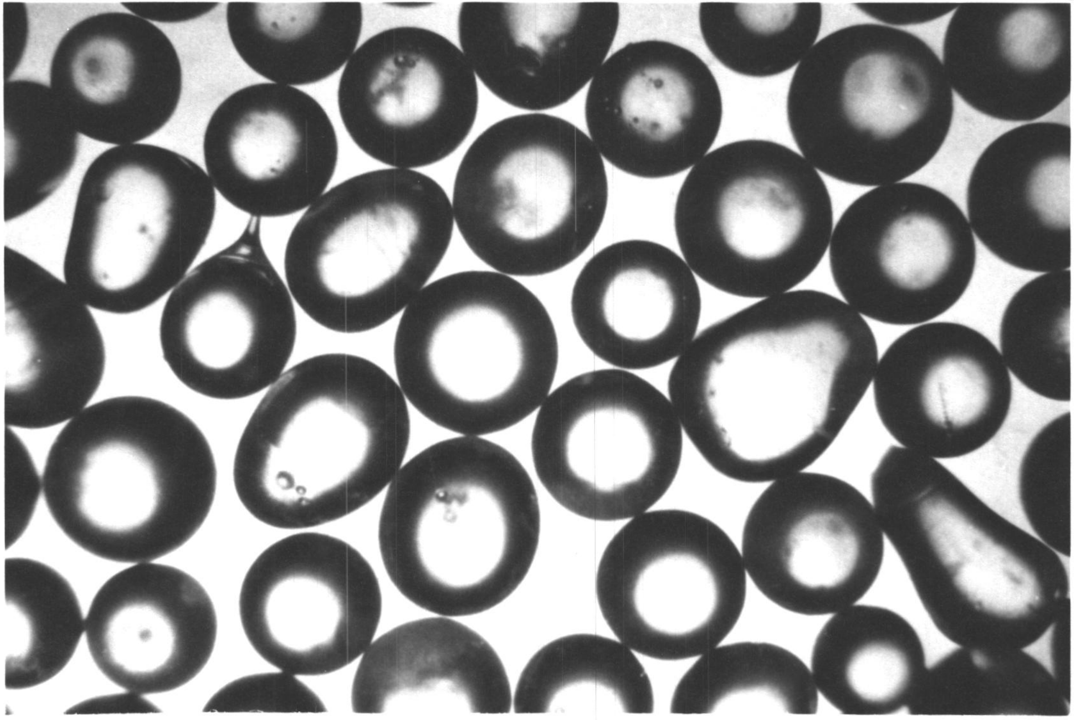

Number 070 Average diameter = 0.0188 inches

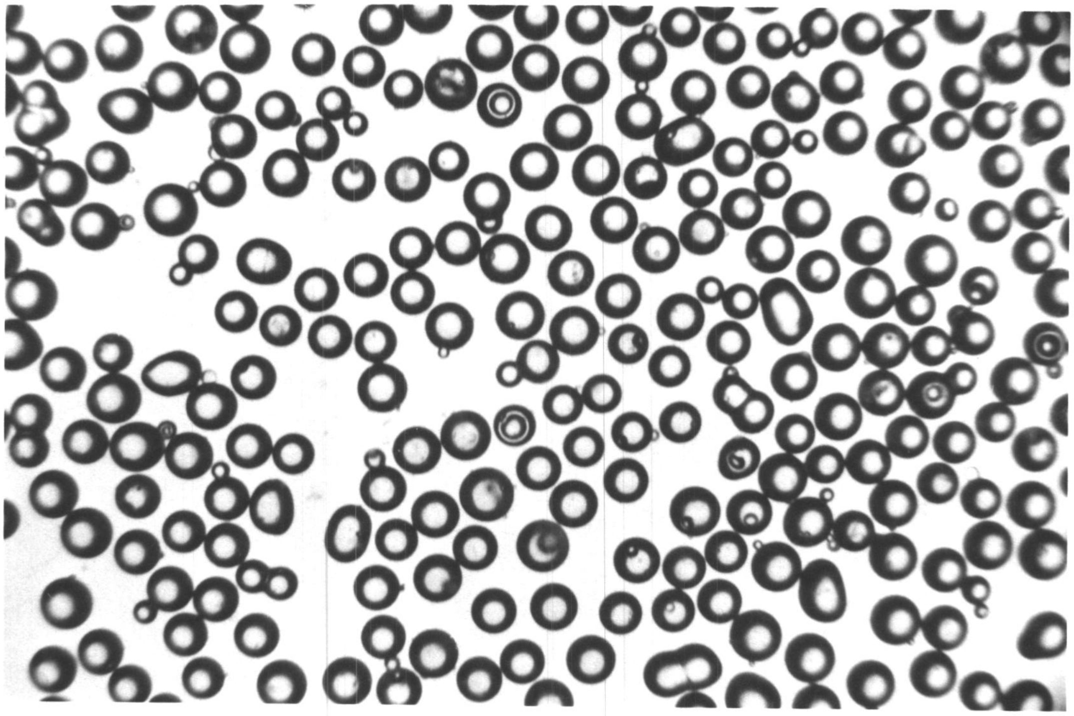

Number 110 Average diameter = 0.0057 inches

Figure 7. Photograph of Glass Beads

each case. For the coarse beads static bed heights of three, nine and 15 inches were studied. The fine bead charges were three, nine, six and 15 inches. The values of particle concentration were determined from measured values of the vertical pressure gradient (10, p. 1107).

Superficial Gas Velocity

Gas velocity was chosen to insure effective fluidization without elutriation. Limitations were also imposed by the blower capacity. Fixed bed conditions were not studied since it was impossible to throttle the turboblower to such a low flow rate. For each amount of coarse beads, three flow rates were investigated. The superficial rates ranged from 850 to 2800 lbs./hr. $ft.^2$ These flow rates varied for the different charges of beads. Two flow rates were investigated for each charge of fine beads. These rates averaged 800 and 1135 lbs./hr. $ft.^2$ It was possible in the case of the fine beads, to use approximately the same flow rates for the different static bed heights. Flow rates measured are within plus or minus ten percent since bed slugging caused variations in the manometer readings.

Heating Surface Location

The tube layout is shown in Figure 3. Since the layout is symetrical, the four numbered positions represent all possible different tube locations. The heating element was studied in each of these four positions for the various bed heights and superficial gas velocities.

The tube wall temperature was observed at several positions along the heating tube. It was found that 11 positions located 1.5, 3.5, 5.5, 11.5, 17.5, 23.5, 29.5, 35.5, 41.5, 43.5 and 45.5 inches from the bottom of the heating element gave sufficient information to obtain the temperature distribution along the length of the tube.

CHAPTER 5

EXPERIMENTAL PROCEDURE

The steps performed in operating the equipment and recording the data are listed in order below.

A. Several preliminary preparations where necessary before starting the equipment

  (1) The stainless steel heating tube was placed in position; the unit rotated to the vertical position and the heating tube connected to the power source.

  (2) The air intake section was secured to the test section.

  (3) The unit was charged with the desired amount of glass beads.

  (4) Ice was placed in the Dewar flask and the thermocouple reference junctions submerged in it.

  (5) The potentiometer was balanced against the internal standard cell.

  (6) The thermocouple probe was moved to the first position in the heating element.

  (7) The heating tube position, particle size and particle charge were recorded.

B. After the preliminary preparations were completed the equipment was operated.

(1) The turboblower was turned on and the desired flow rate obtained.

(2) The direct current power source was turned on.

(3) The recorder was turned on and the thermocouple switch set to read probe temperature.

(4) After steady-state had been reached, usually in 30 minutes, the following were recorded:

   (a) Voltage

   (b) Current

   (c) Inlet and outlet air temperature

   (d) Probe temperature

   (e) Pressure drop and orifice manometer readings

   (f) Manometer board temperature

(5) The temperature probe was then moved to a new position and the readings repeated when steady state had been reached. Steady state was reached in 5 to 15 minutes depending upon the position, and was observed using the automatic recorder.

(6) After the 11 probe positions had been studied the power was turned off and the bed and heating tube allowed to cool off.

C. At the completion of the steps in B, the probe was returned to position one and steps A-4, 5, 6, 7, and B repeated for the various flow rates for the particular solids charge.

D. At the completion of step C, the unit solids charge was changed and steps A-3, 4, 5, 6, 7, B and C repeated for the different solids charges.

E. At the completion of step D the unit was emptied of solids and placed in a horizontal position.

  (1) The heating tube was placed in a new position and steps A, B, C, and D repeated for all four heating tube locations.

F. At the completion of step E, steps A, B, C, D, and E were repeated for the other particle size.

CHAPTER 6

SAMPLE CALCULATIONS

To illustrate the calculations involved, a set of sample calculations for one run is presented below.

Flow Rate

The equation for calculating the flow rate from the pressure drop across a square-edged circular orifice is (15, p. 405)

$$w = q_1 \rho_1 = C \; Y \; S_2 \sqrt{\frac{2 \; g_c \; (P_1 P_2) \; \rho_1}{1 - \beta^4}}$$

where

w = mass flow rate, lb_m/sec

q_1 = volume flow rate at upstream pressure and temperature, ft^3/sec

ρ_1 = density at upstream pressure and temperature, lb_m/ft^3

g_c = 32.1740

S_2 = cross sectional opening at orifice, ft^2

P_1, P_2 = pressure at upstream and downstream taps, lb_f/ft^2

C = coefficient of discharge

Y = expansion factor

The expansion factor Y for a square-edged circular orifice is given by $$Y = 1 - \frac{(\rho_1 - \rho_2)}{P_1 K} (0.41 + 0.35\ \beta^4)$$

$K = C_p/c_v$

β = ratio of the orifice diameter to pipe diameter .

An inclined manometer was used to measure the pressure drop across the orifice, therefore

$$P_1 - P_2 = \frac{g_c}{g} \frac{(R-R_o)\ (62.37-.074)\ \sin 30}{30.5}$$

where R and R_o are the manometer reading in centimeters. For a manometer reading of 1.4 centimeters

$$P_1 - P_2 = 1.4\ \frac{(62.37-.074)}{30.5}\ .5 = 1.42\ lb_f/ft^2$$

therefore

$$Y = 1 - \frac{1.42}{1.4 x 2120} \quad 0.41 + 0.35\ (.1897)$$

$$Y = .99978 \approx 1$$

As a first assumption C is taken equal to .61

$$q = \frac{.61 \times 0.0218}{.074} \sqrt{\frac{2 \times 32.174\ (1.42)\ .074}{1 - .1897}}$$

$$q = .538\ ft^3/sec$$

at 83° F. viscosity of air = .0186 centipoise

density of air = .074 lbs/ft^3

$$N_{Re} = \frac{dG}{\mu} = \frac{.25 \times .538 \times .074 \times 3600}{.0186 \times 2.42 \times .0513} = 15,500$$

For a Reynolds number of 15,500 the coefficient of discharge is equal to .61 and no further calculations are necessary.

Heat Flux

The electrical power input was calculated as the product of the measured voltage and current since the power factor was unity. The heat transferred to the fluidized bed from the heating element was considered equal to the power input with minor corrections for heat losses in the lead wires. An example follows:

Measured voltage = 2.65 volts

Measured current = 36.5 amps

Power = ei = 96.7 watts

Resistance of number six copper wire = .395 ohms/1000 feet

Power loss = $i^2r = (36.5)^2 \times \frac{395}{1000} \times 10 = 5.25$ watts

Actual power input = 96.7 - 5.3 = 91.4 watts

1 Btu = 0.293 watt-hr

therefore

power input = 312 Btu/hr

area of heating element = .982 ft^2

Heat flux = 312 x 1/.982 = 318 Btu/hr ft^2

Temperature Measurement

All temperatures were measured using thermocouples, and perliminary calculations involved converting emf readings to temperature by means of standard conversion tables. The thermocouples were calibrated, against a thermometer accurate to 0. 2° F, up to a temperature of 116°F.

A heat balance for the sample run shows a substantial rise in the bulk temperature of the air.

$$Q/A = 318 \text{ Btu/hr ft}^2$$

$$w = 145 \text{ lbs/hr}$$

$$T_{in} = 82.7^\circ \text{ F}$$

$$cp = .240 \text{ Btu/lb } ^\circ\text{F}$$

$$Q/A = wC_p (T_{out} - T_{in})$$

$$318 = 145 \times .240 (T_{out} - 82.7)$$

$$T_{out} = 91.8^\circ \text{ F}$$

The temperature difference measured was based on tube wall temperature and air inlet temperature. The temperature difference based on the local bulk temperature of the air was calculated

$$T_w - T_{b_{loc}} = T_w - (T_{in} + \frac{Q/A}{wC_p} \frac{x}{L})$$

where L = heating tube length

x' = position along heating tube

An example follows,

At 23.5 inches from the heating tube bottom

$$T_w = 103.8$$

$$(T_w - T_{in}) = 20.4 \text{ F°}$$

$$(T_w - T_{b_{loc}}) = 20.4 - \frac{318}{145 \times .240} \quad \frac{23.5}{45.5}$$

$$(T_w - T_{b_{loc}}) = 15.7 \text{ °F}$$

Heat Transfer Coefficient

$$Q/A = h_{loc} (T_w - T_{b_{loc}})$$

$$318 = h_{loc} (15.7)$$

$$h_{loc} = 20.2 \text{ Btu/hr ft}^2 \text{ F°}$$

Bed Density

The values reported for bed density are the measured values of the vertical pressure gradient. This is a good approximation for batch fluidization (10, p. 1107).

$$\Delta P = L_f (1 - \epsilon) (\rho_s - \rho_f) \frac{g_c}{g}$$

L_f = bed height, ft

ϵ = fraction voids

ρ_s = solid density, lb/ft^3

ρ_f = fluid density, lb/ft^3

Δ_ρ = pressure drop lb$_f$/ft^2

The bed density is $\rho_s (1-\epsilon)$

for this example

Section	Pressure drop, lb$_f$/ft^2
1	12.4
2	6.1
3	4.8

$$12.4 = .917 (1-\epsilon) (156-.074) \; g_c/g$$

$$(1-\epsilon) = .087$$

Bed density = $156 \times .087 = 13.6$ lbs/ft^3

$$6.1 = .917 (1-\epsilon) (156-.074) \; g_c/g$$

$$(1-\epsilon) = .043$$

Bed density = $156 \times .043 = 6.65$ lbs/ft^3

$$4.8 = .917 (1-\epsilon) (156-.074) \; g_c/g$$

$$(1-\epsilon) = .034$$

Bed density = $156 \times .034 = 5.24$ lbs/ft^3

Subsequent Calculations

Several additional calculations were required for a complete analysis of the data.

Arithmetic average heat transfer coefficients for heat transfer from the tube to the fluidized bed were calculated.

The Nusselt Number based on tube diameter was calculated from the average heat transfer coefficient.

The Reynolds Number based on equivalent diameter was calculated from the flow rate.

Calculations of heat transfer coefficients for a segmentally baffled heat exchanger of the same dimensions were made (4).

Power losses in the heat exchanger were calculated for the unbaffled case, the fluidized bed case, and the baffled case.

CHAPTER 7

ANALYSIS OF RESULTS

Heat Transfer Coefficient for Air

In Figure 8 the local heat transfer coefficient for air alone is plotted as a function of the distance along the heating tube measured as inches from the entrance. The data shown are for tube location 1, indicated in Figure 3. Also shown are the data of Ambrose (1, p. 125) for an unbaffled exchanger with a six inch shell containing four, 1.0 inch tubes. Ambrose's coefficients are somewhat higher for several reasons: he measured point temperatures on a nichrome resistance ribbon mounted on a plastic rod; the air entered his exchanger normal to the tubes whereas in this work it entered parallel to the tube bundle; the equivalent diameter of four, 1.0 inch tubes in a six inch shell is considerably greater than that of 19, 3/4 inch tubes in the same size shell, resulting in significantly higher Reynolds numbers. The values of the local coefficients obtained in this work decreased approximately 69 percent over the length of the exchanger as compared to a 80 percent reduction for the coefficients obtained by Ambrose.

The average heat transfer coefficients for the various tube locations are plotted as a function of Reynolds number in Figure 9.

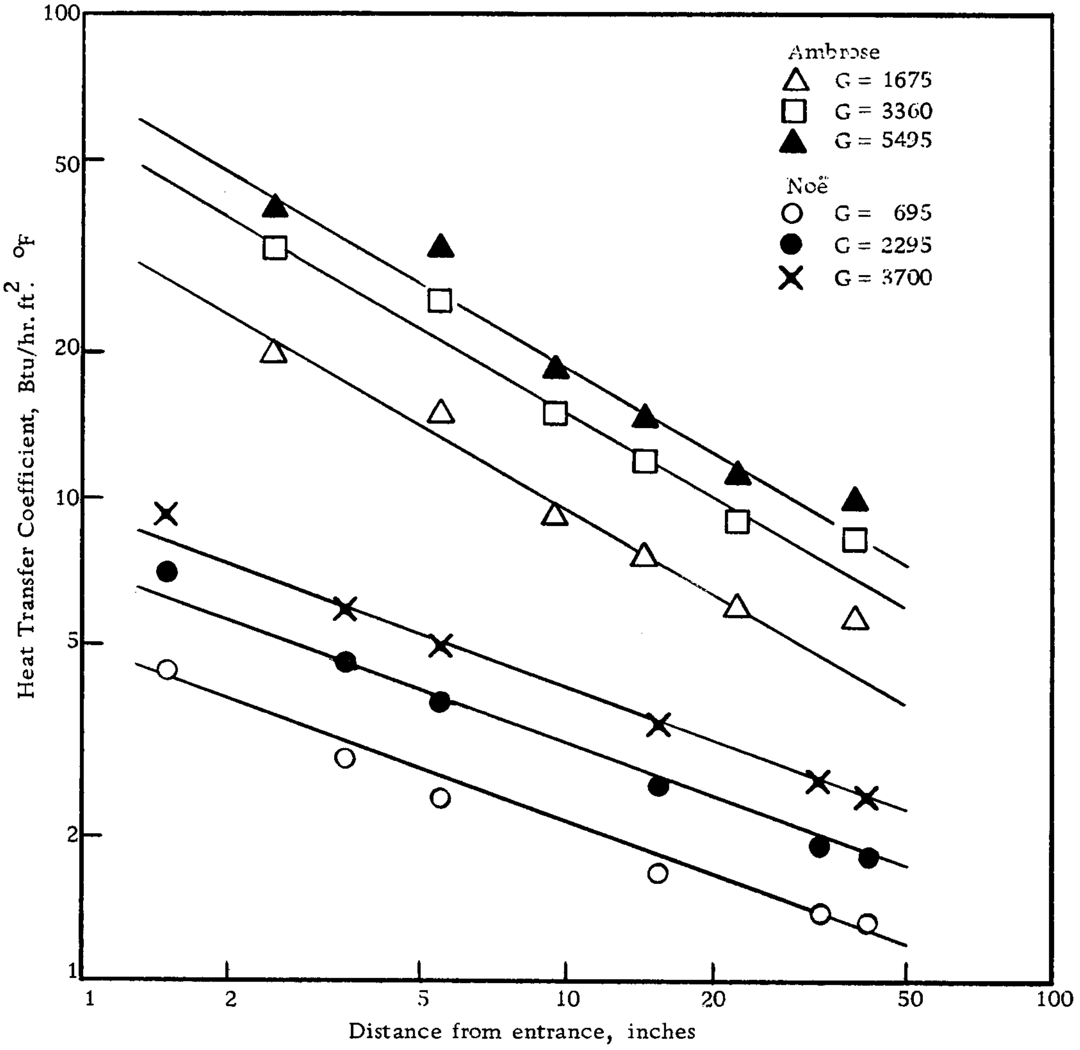

Figure 8. Local Heat Transfer Coefficient for Air

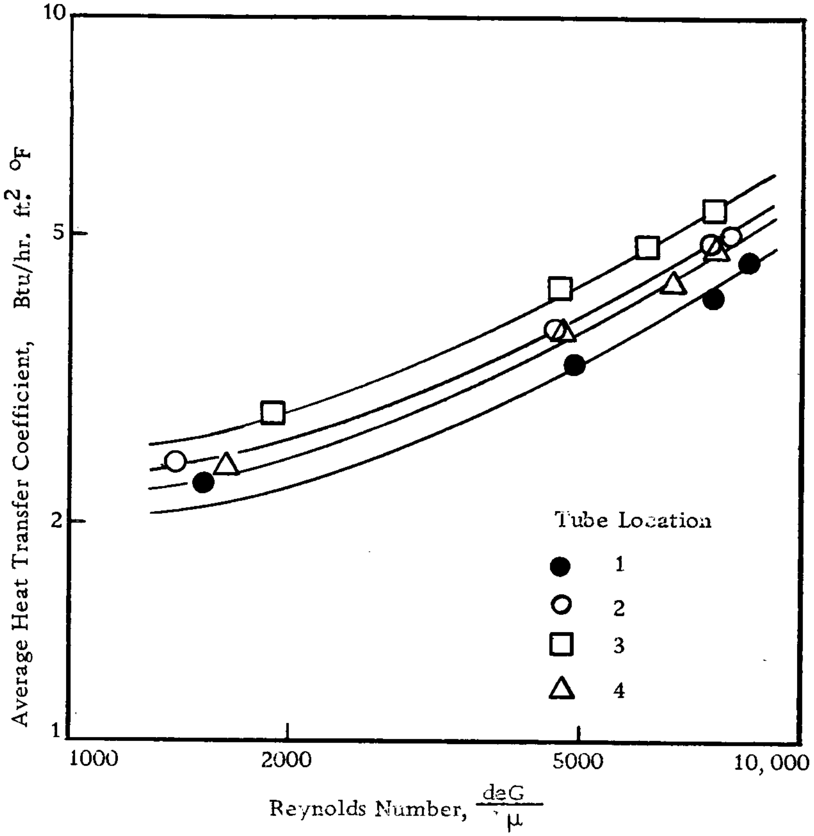

Figure 9. Average Heat Transfer Coefficient for Air

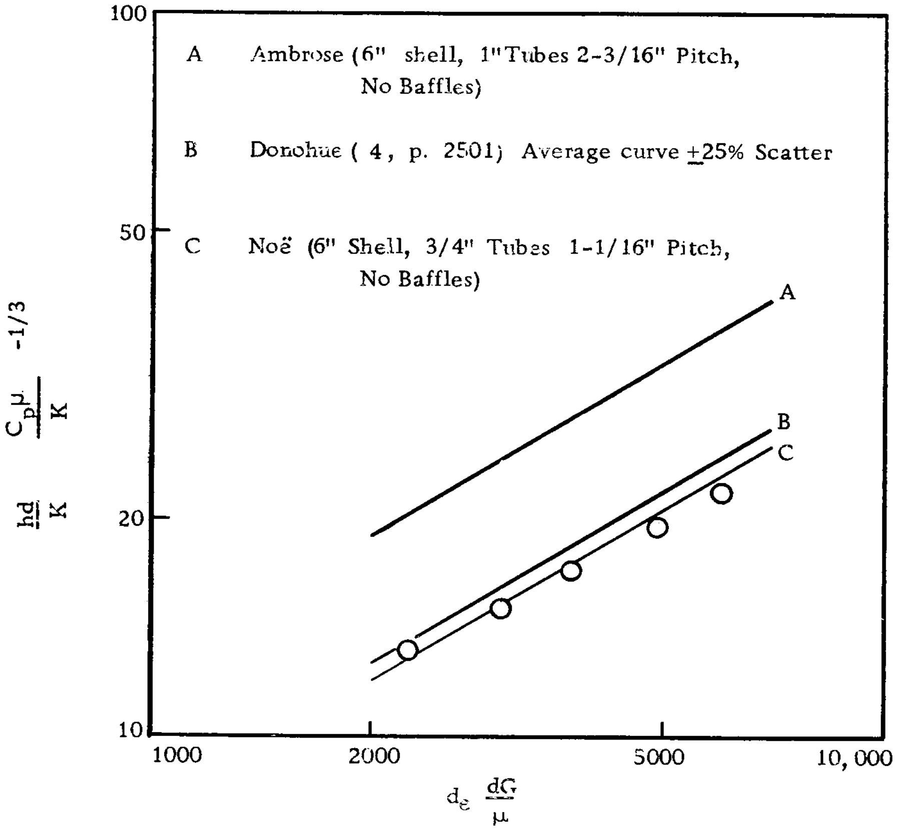

Figure 10. Heat Transfer Rate in An Unbaffled Exchanger

Tube location 1 produced the lowest values of the coefficients since the air flow about it is less turbulent; due to channeling it flows at a lower velocity, than in other parts of the exchanger. Variations in the coefficients for tube locations 2, 3 and 4 may be attributed to shell wall effects.

The term $\left(\frac{hd}{k}\right)\left(\frac{C_p\mu}{k}\right)^{-1/3}$ was calculated from the arithmetic average Nusselt number and the Prandtl number of air which was taken as 0.71 in all cases. In Figure 10 this dimensionless term is plotted as a function of $d_e\left(\frac{dG}{\mu}\right)$ in order to compare with a correlation proposed by Donohue (3, p. 2501). An extrapolation of Ambrose's data was also used for comparison. Donohue's curve represents experimental data with a maximum deviation of 25 percent about it. The data for the present work lie within this range and have the characteristic 0.6 slope. The results indicate good agreement with the correlation of Donohue and also show that the measured coefficients have reasonable values.

Effect of Glass Beads

The addition of fluidized glass beads caused a significant increase in the heat transfer coefficient. The effect of 0.0057 inch diameter beads having a static bed height of nine inches for heating tube location 2 is shown in Figure 11. Similar plots for three, six,

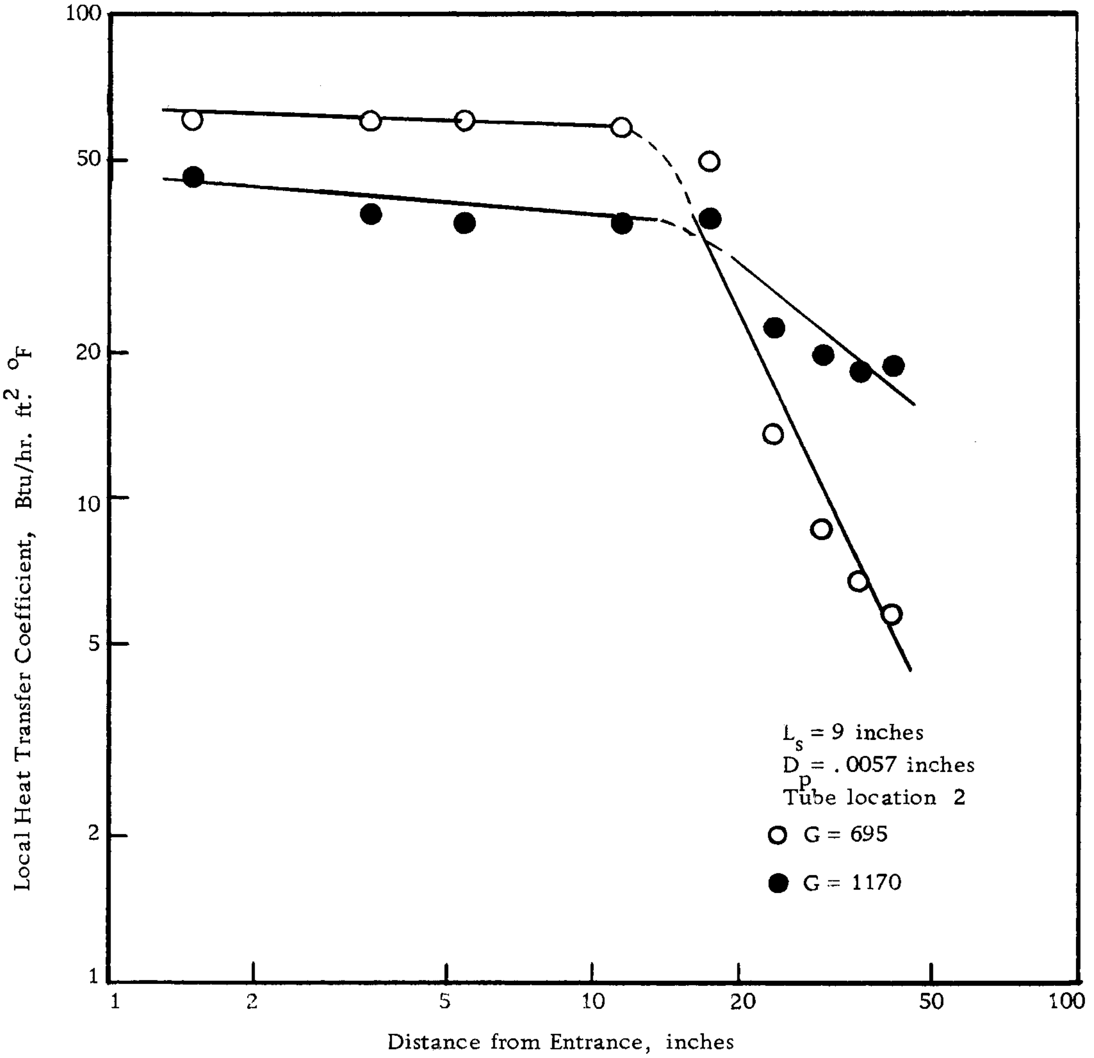

Figure 11. Local Heat Transfer Coefficient for Fluidized Bed

nine, and 15 inch bed heights of fine and coarse beads for tube location 2 are presented in the appendix. In all cases the curves are similar in shape. A comparison of Figure 11 with Figure 8 indicates a 4- to 13-fold increase in the heat transfer coefficient due to the presence of fluidized glass beads. The local coefficient is fairly constant up to approximately 11.5 inches from the entrance and then decreases sharply thereafter. Visual observation indicated that the bed density changed markedly at this point and presssure losses also indicated this density change.

It is also interesting to note that the local heat transfer coefficient is higher at the lower flow rate in the dense section of the bed. Visual observation indicated that a more uniform fluidization in the dense section of the bed was obtained with the lower flow rate, whereas slugging and large gas bubbles were more evident at the higher flow rate.

In the sparse section of the bed, beyond 11.5 inches from the entrance, the local heat transfer coefficient is higher for the higher flow rate as is the case for heat transfer to single phase fluids. Visual observation of this section of the bed showed no perceptible change with flow rate, however pressure losses indicated some variation of bed density with flow rate.

These results indicate that the local heat transfer coefficient in the dense section of the bed depends upon the nature of fluidization, higher coefficients being obtained when the bed is uniformly fluidized and not filled with large gas bubbles.

Effect of Heating Tube Location

For the fluidized bed, the effect of heating tube location on the local heat transfer coefficient is shown in Figure 12. Greater variation between tube location occurs in the dense section of the bed and with the larger static bed height as indicated in Figure 12. The curves are drawn through the average value for all tube locations. In most cases tube location 1 produced the lowest values of the local coefficients while tube location 3 produce the highest values. When the arithmetic average coefficients for the entire length of the tube are considered, the values do not differ significantly with tube location since the local coefficients do not differ significantly in the upper 75 percent or less dense section of the bed.

Effect of Solids Concentration

Figure 13 shows the variation of the arithmetic average heat transfer coefficient for the whole tube bundle as a function of the solids concentration. The variation of the heat transfer coefficient

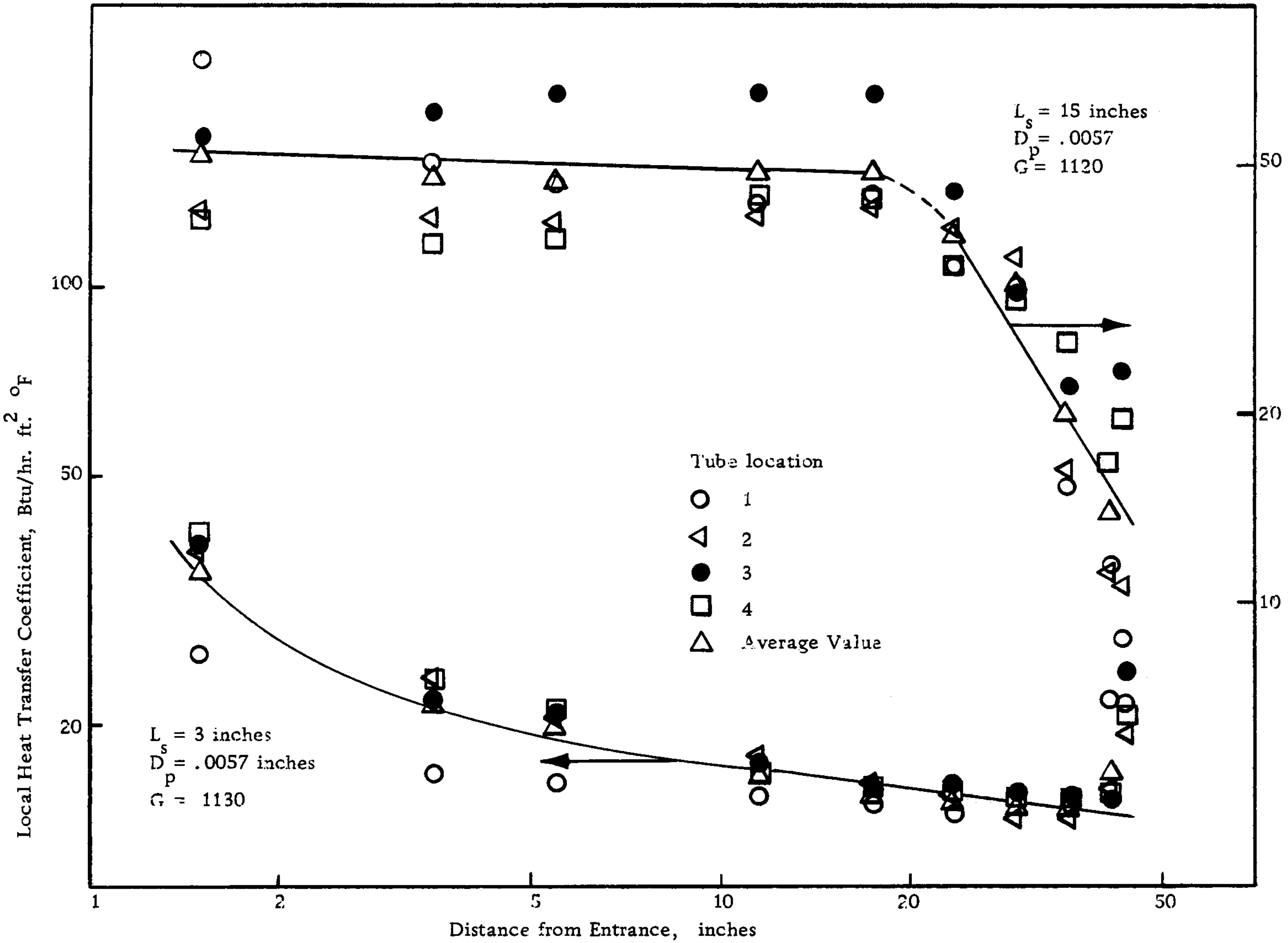

Figure 12. Effect of Heating Tube Location on Local Heat Transfer Coefficient

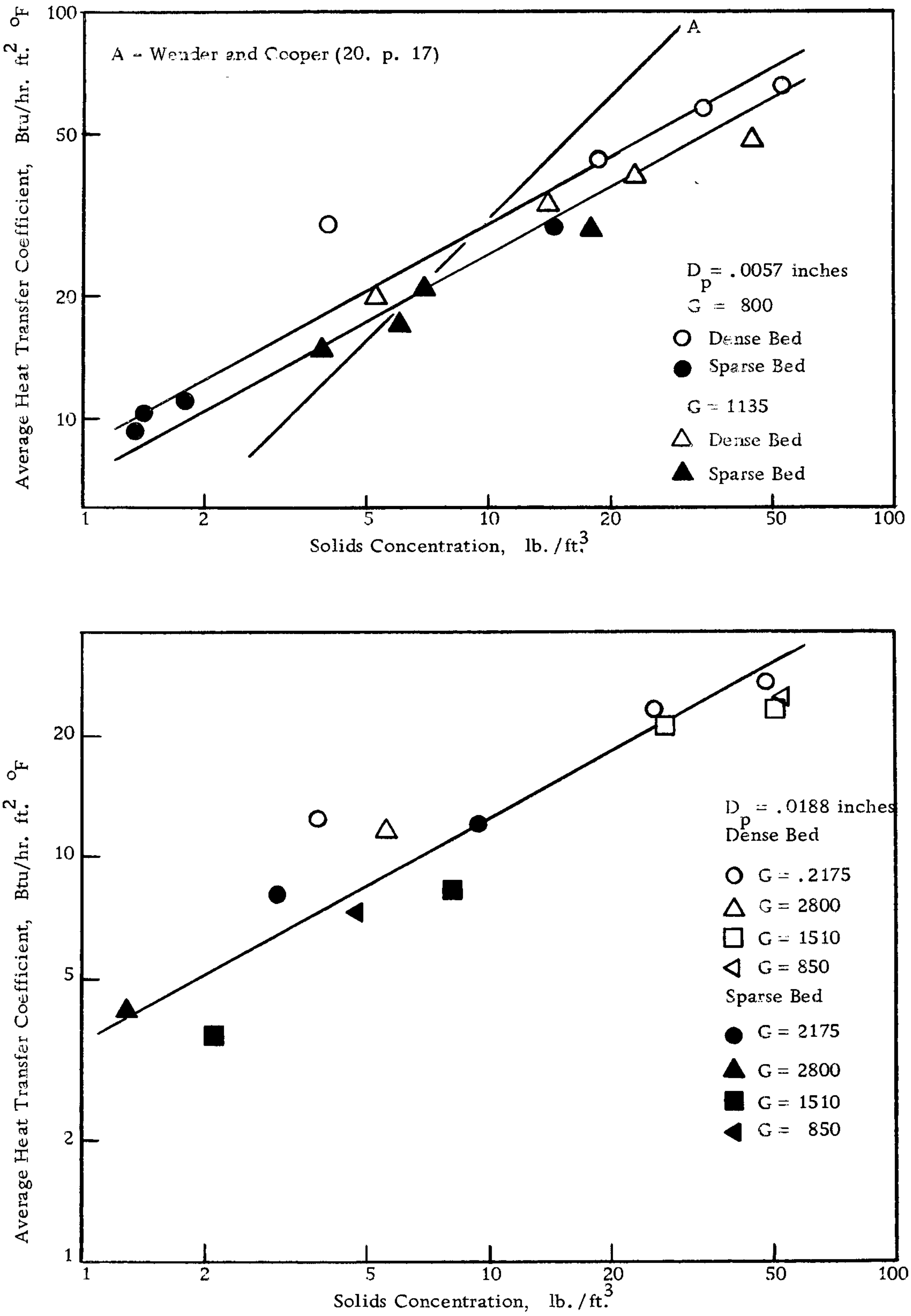

Figure 13. Variation of Average Heat Transfer Coefficient with Solids Concentration

with bed density as predicted by Wender and Cooper (20) for single tubes is also shown. The average solid concentration is obtained from the measured pressure drop over three sections of the bed.

The average coefficient increases with increasing flow rate for the fine beads whereas it is essentially independent of flow rate for the coarse beads. While the data do not agree exactly with the correlation of Wender and Cooper for a flow rate of 800 lbs/hr ft^2 since it is for single tubes rather than a tube bundle, the magnitudes of the coefficients agree for bed densities ranging from 2 to 20 lbs/ft^3.

The arithmetic average heat transfer coefficient as a function Reynolds number is shown in Figure 14 for coarse beads. Again it is seen that the coefficient is much higher in the dense section of the bed as shown by the graph on the right. The average coefficient was found to be higher for the fine beads, however not enough flow rates were studied for a true comparison. Figure 14 also shows the approximate independence of heat transfer coefficient of flow rate for the coarse beads.

Power Requirements and Space Requirements

Any increase in heat transfer coefficient brings about an increase in the capacity of the exchanger. If this increase is

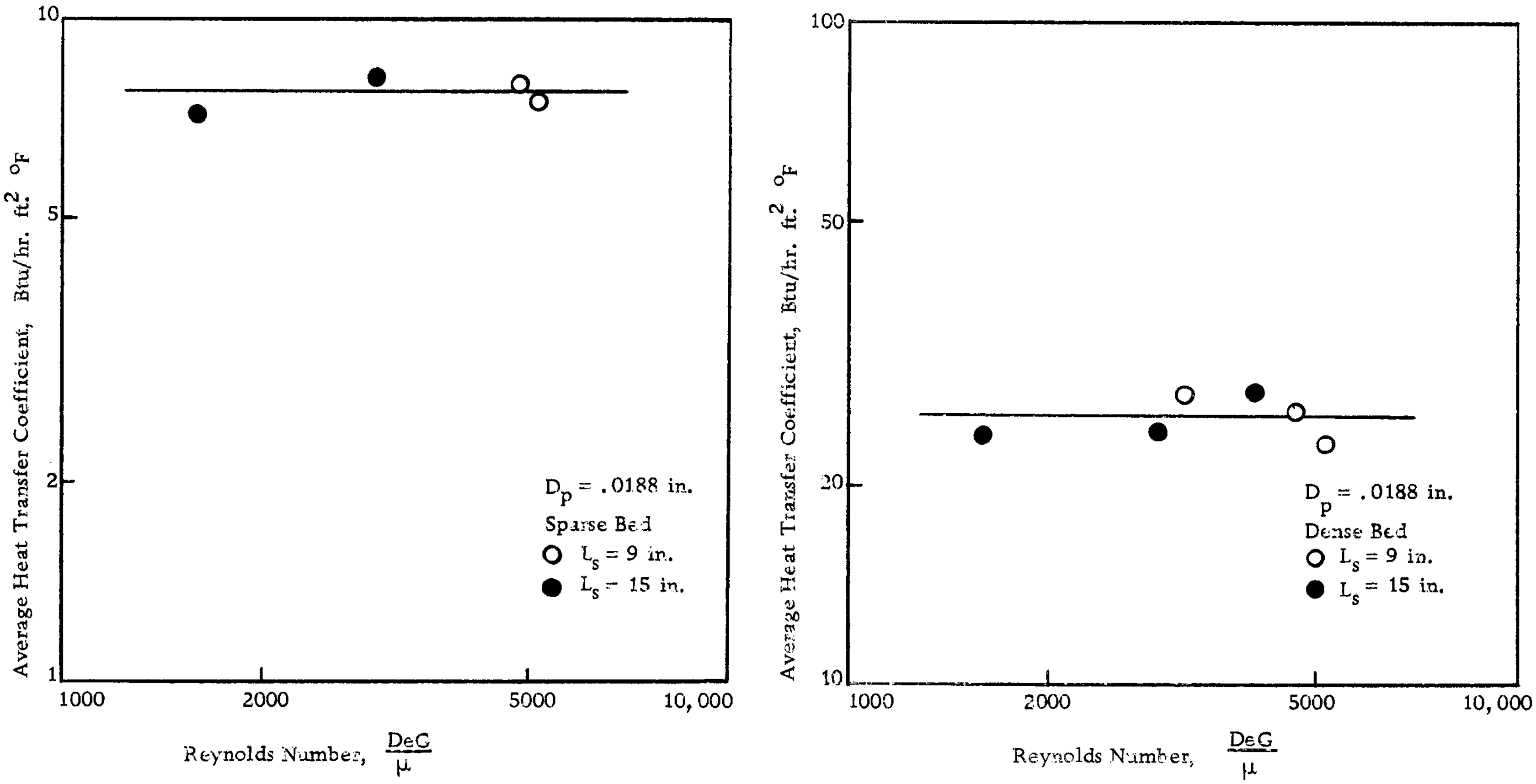

Figure 14. Variation of Average Heat Transfer Coefficient with Reynolds Number

accompanied by an increase in pumping power the actual cost of the extra capacity may not be economical. In situations where power is an important factor the ratio of heat transfer capacity to pumping power will be important. On the other hand if space is the important factor any increase in heat transfer capacity will be advantageous.

Calculations were carried out to compare the pumping power requirements and capacity of the fluidized bed heat exchanger studied in the present work with a unit of the same tube configuration and dimensions but containing 10, 25 percent cut, segmental baffles.

The ratio of the pressure drop across the bed containing fine beads to that of the empty unbaffled exchanger is shown as a function of static bed height in Figure 15; the ratio of the pressure drop across the fluidized bed to that across a segmentally baffled exchanger is also plotted as a function of static bed height. This ratio is as high as 5000 for the unbaffled exchanger as compared to 17 for the baffled unit. Below a static bed height of three inches this ratio is less than unity for the baffled exchanger.

The ratio of the heat transfer capacity, hA, to the pumping power requirement as calculated from the pressure drop across the bed is shown as a function of the static bed height in Figure 16. The upper left corner shows this ratio for a solids concentration of zero, i.e. an unbaffled exchanger. It is evident that if power costs are

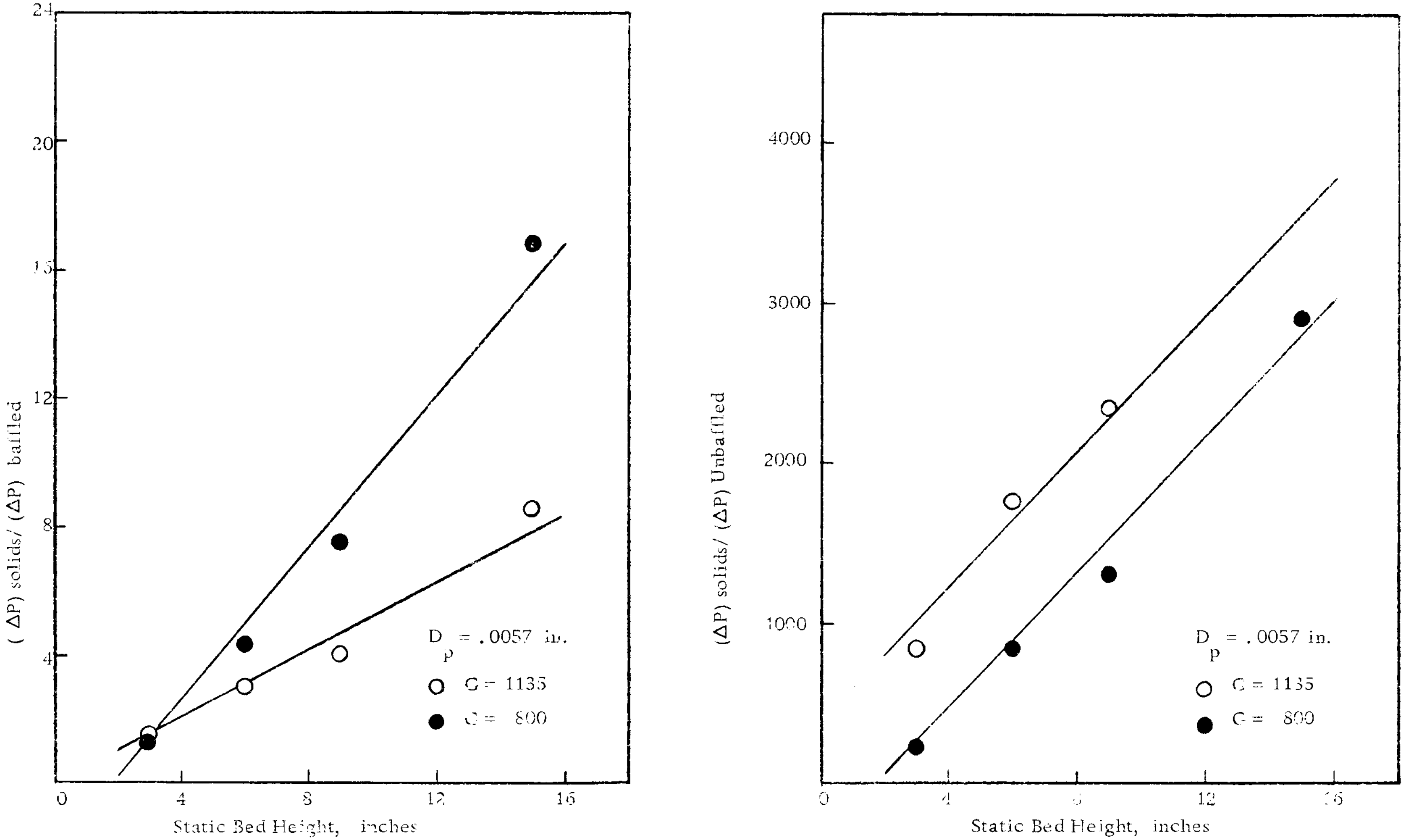

Figure 15. Variation of Pressure Drop Ratio with Static Bed Height

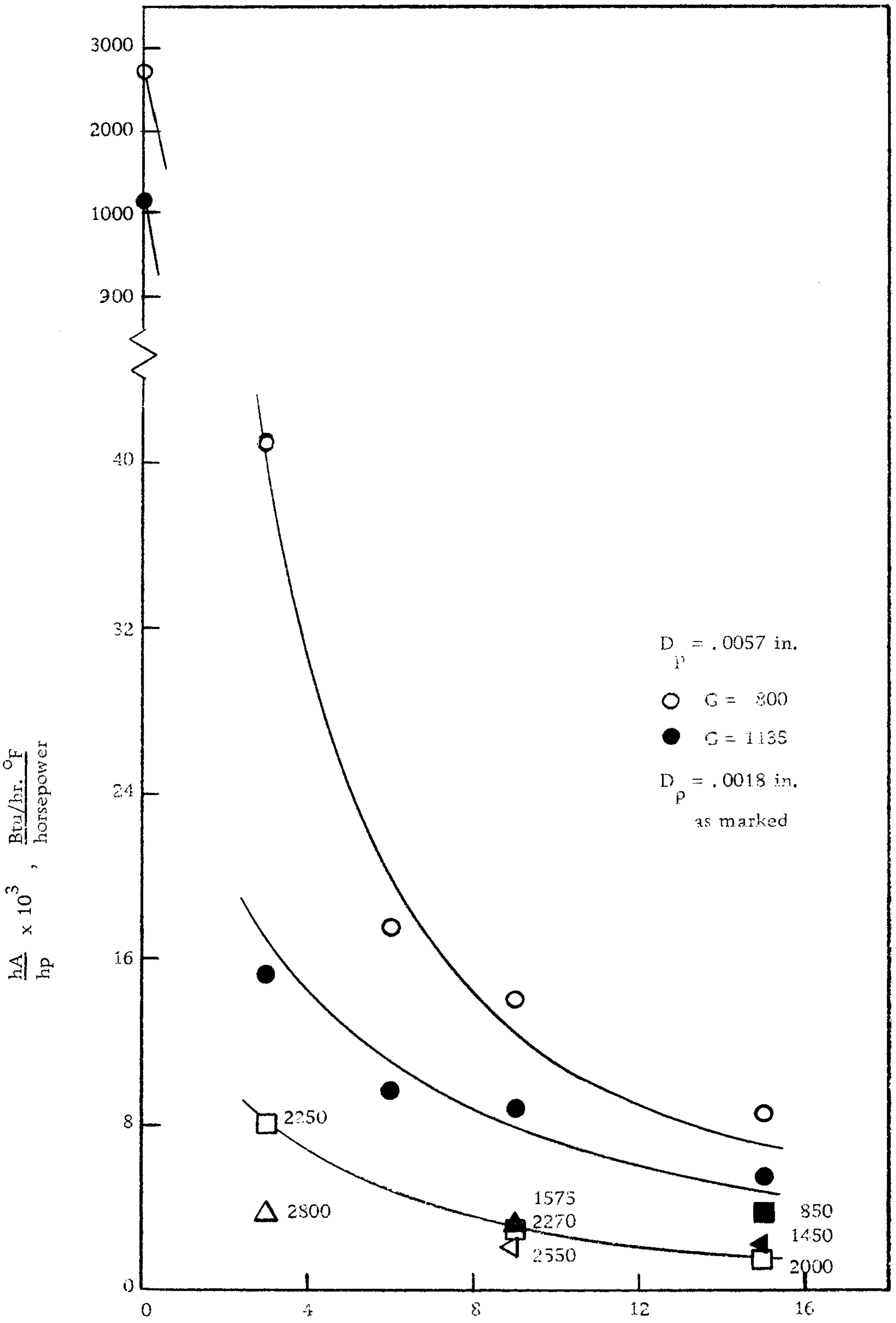

Figure 16. Heat Transfer Duty per Horsepower Requirement: Variation with Static Bed Height

important the fluidized bed heat exchanger offers no advantage over the unbaffled exchanger, however the low coefficients of unbaffled heat exchangers require that they be excessively large if capacity is to be of reasonable magnitude. It is for this reason that baffled exchangers are used and hence comparison is made with a baffled exchanger.

Figure 17 shows the ratio of the heat transfer capacity for the fluidized bed exchanger to that of the unbaffled and baffled exchangers as a function of static bed height. A significant increase in heat transfer is obtained with the fluidized bed exchanger, increasing with increasing static bed height. At a static bed height of six inches and a flow rate of 800 lbs/hr ft^2, 1/9 the heat transfer area of an unbaffled exchanger and 1/3 the area of a baffled exchanger is required for equal capacity by a fluidized bed exchanger. Therefore, in both cases, the fluidized bed exchanger shows a definite advantage in terms of space requirement alone.

The ratio hA/horsepower for the fluidized bed exchanger to hA/horsepower for the baffled exchanger is shown as a function of static bed height in Figure 18. When this ratio exceeds unity the fluidized bed exchanger is better both from a standpoint of space and power requirement than the baffled exchanger. This occurs at bed heights less than five inches.

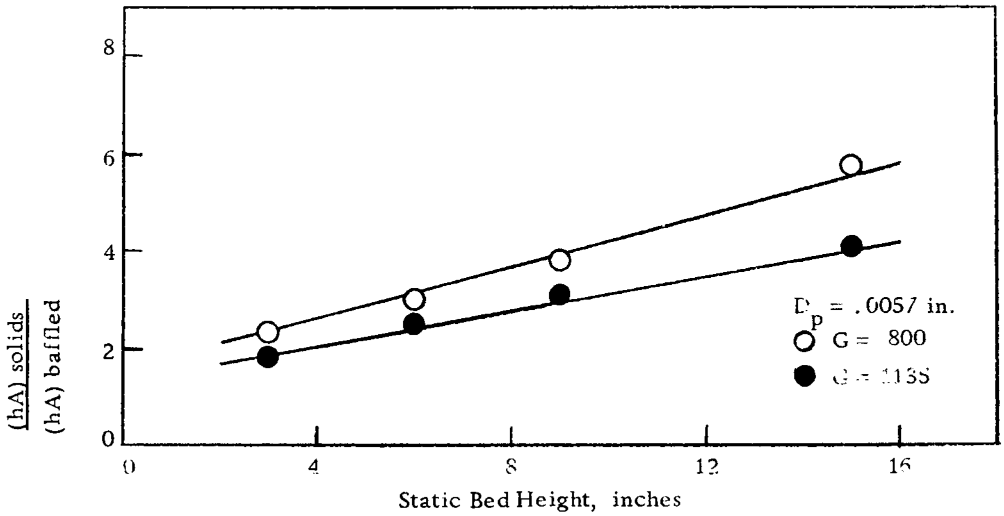

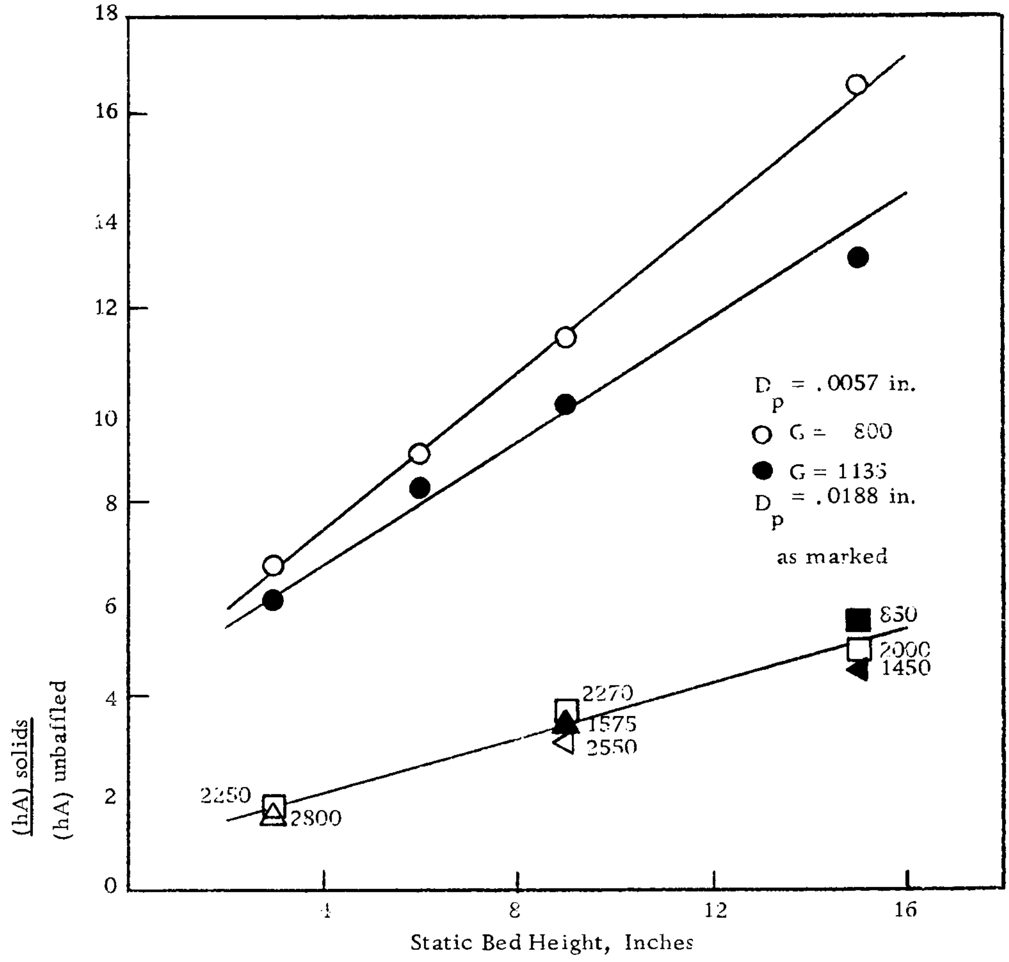

Figure 17. Variation of Heat Transfer Duty Ratio with Static Bed Height

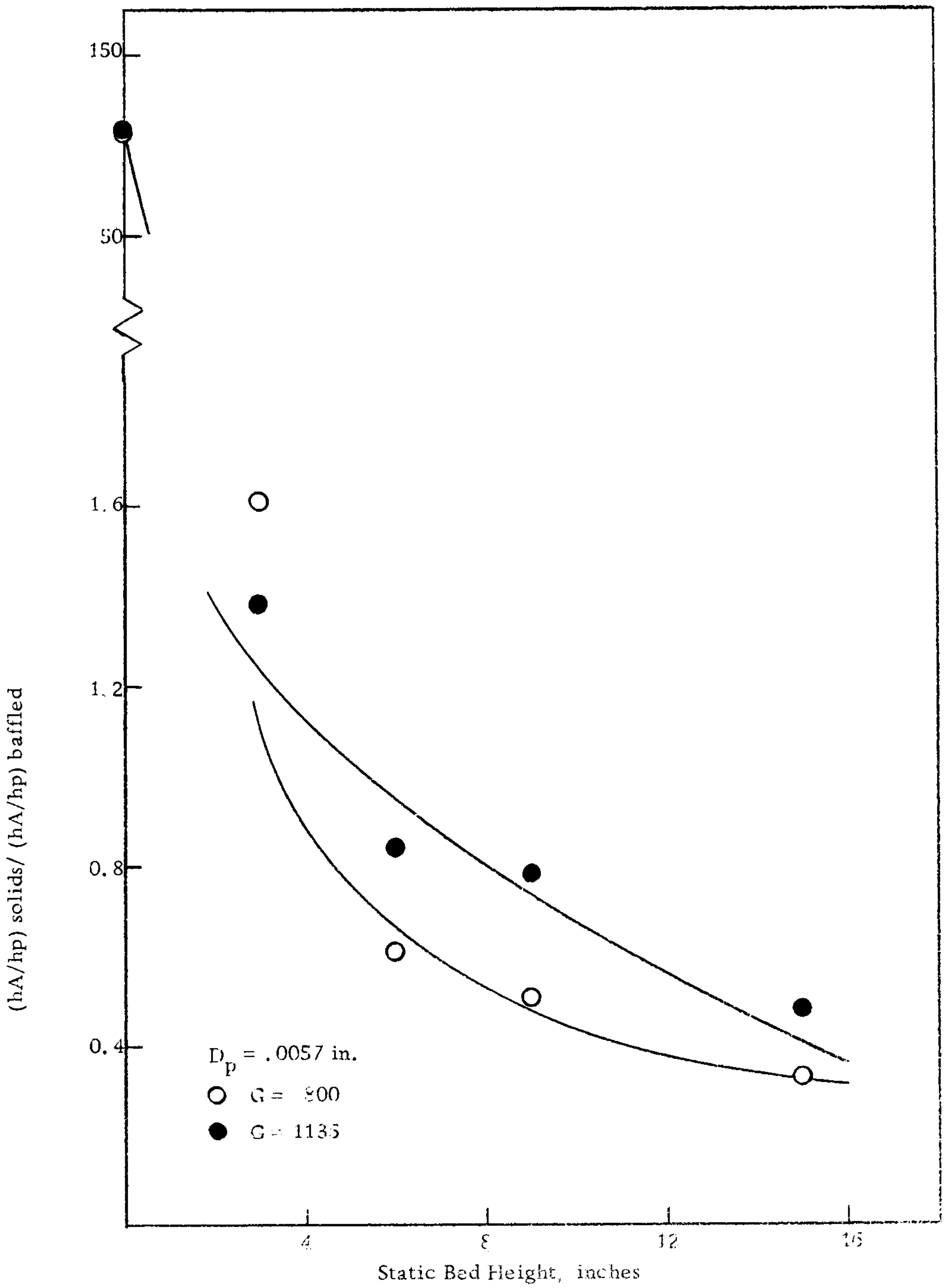

Figure 18. Heat Transfer Duty per Horsepower Requirement Ratio: Variation with Static Bed Height

CHAPTER 8

RESULTS AND CONCLUSIONS

Local and average heat transfer coefficients for heat transfer from internal tubes to a fluidized bed of glass beads and air have been investigated. The effects of heating tube location, particle size and concentration, and air flow rate were determined. The following results and conclusions are obtained from the data.

The average heat transfer coefficients for air alone agreed with accepted correlations (3, p. 2501) and it is concluded that correct coefficients were measured.

The addition of fluidized glass beads to the heat exchanger resulted in significant increases in the local heat transfer coefficient (at the same position) ranging from 1.5- to 50-fold. The arithmetic average heat transfer coefficients were increased as much as 25-fold. The increase was greatest in the lower, more dense section of the bed. Local coefficients were nearly independent of distance from the entrance in this dense region.

For the fine beads, local heat transfer coefficients decreased with increasing flow rates in the dense section of the bed but for the coarse beads were nearly independent of flow rate. In the sparse section, local coefficients increased with flow rate similar to their variation for single phase flow.

Tube location did not greatly affect the average coefficients, however significant variations did occur among the local coefficients at various locations on a cross section in the dense portion of the bed.

Average heat transfer coefficients increase as a power function of solids concentration and values obtained agree in magnitude with those of accepted correlations (20).

Power requirements for a fluidized bed heat exchanger are considerably greater than those for unbaffled and segmentally baffled heat exchangers.

Heat transfer capacity per unit of pumping power is less for the fluidized bed exchanger than for the unbaffled and baffled cases and decreases with increasing static bed height.

The ratio of the heat transfer capacity of the fluidized bed exchanger to that of the unbaffled and baffled exchangers is considerably greater than unity and increases with increasing static bed height. Thus less heat transfer surface area is required in the fluidized bed exchanger and it is therefore a more compact exchanger for a given capacity.

The ratio of heat transfer capacity per unit of pumping power for the fluidized bed exchanger to that of the baffled exchanger is greater than unity up to a static bed height of five inches. Therefore it is concluded that a fluidized bed heat exchanger containing fine glass beads with a bed height less than five inches would be economically advantageous over the conventionally baffled exchanger. This comparison does not consider construction costs of the two exchangers.

CHAPTER 9

RECOMMENDATIONS

This investigation was exploratory in nature, hence many variables of fluidized bed heat exchange remain to be studied. Several proposals for continuing study are made below.

Slight modification of the existing equipment would permit a greater range of flow rates and initial bed concentrations to be studied.

An investigation of solids other than glass spheres such as catalyst particles or metal powders would illustrate the effect of particle geometry and composition on the heat transfer.

Study of a different tube size and pitch should be made to determine the effect on heat transfer.

It is recommended that a fluidizing medium other than air, such as water, be studied since it would provide valuable information for actual utilization of a fluidized bed heat exchanger.

Solids and fluidizing media which cause scale and dirt deposits should be studied to determine the effect of fouling on fluidized bed heat transfer.

BIBLIOGRAPHY

1. Ambrose, Tommy W. Local shell-side heat transfer coefficients in baffled tubular heat exchangers. Ph. D. Thesis. Corvallis, Oregon State College, 1957. 185 numb. leaves.

2. Bischoff, K. Axial thermal conductivity in packed beds. Canadian Journal of Chemical Engineering 40:161-163. 1962.

3. Donohue, Daniel A. Heat transfer and pressure drop in heat exchangers. Industrial and Engineering Chemistry 41:2499-2511. 1949.

4. Donohue, Daniel A. Heat exchanger design: part three. Petroleum Refiner 34(11):175-184. 1955.

5. Frantz, Joseph F. Fluid to particle heat transfer in fluidized beds. Chemical Engineering Progress 57(7):35-42. 1961.

6. Frantz, Joseph F. Design for fluidization. Chemical Engineering 69(21):89-96. 1962.

7. Gopalarathnam, C., H. Hoelscher and G. Laddha. Effective thermal conductivity in packed beds. A. I. Ch. E Journal 7:249-253. 1961.

8. Gupta, A. S. and G. Thodos. Mass and heat transfer in the flow of fluids through fixed and fluidized beds of spherical particles A. E. Ch. E. Journal 8:608-616. 1962.

9. Knudsen, James G. and D. L. Katz. Fluid dynamics and heat transfer. New York, McGraw-Hill, 1958. 576 p.

10. Lewis, W. K., E. R. Gilliland and W. C. Bauer. Characteristics of fluidized particles. Industrial and Engineering Chemistry 41:1104-1117. 1949.

11. Lewis, W. K., E. R. Gilliland and H. Girouard. Heat transfer and solids mixing in beds of fluidized solids. Chemical Engineering Progress Symposium Series 58(38):87-97. 1962.

12. McAdams, William H. Heat transmission. 3rd ed. New York, McGraw-Hill, 1954. 532 p.

13. McCabe, W. L. and J. C. Smith. Unit operations of chemical engineering. New York, McGraw-Hill, 1956. 945 p.

14. Mickley, Harold S. and Charles A. Trilling. Heat transfer characteristics of fluidized beds. Industrial and Engineering Chemistry 41:1135-1147. 1949.

15. Perry, J. H. Chemical engineers' handbood. 3rd ed. New York, McGraw-Hill, 1956. 1942 p.

16. Richardson, J. F. and J. W. Smith. Heat transfer to liquid fluidized systems and to suspensions of coarse particles in vertical transport. Transactions of the Institution of Chemical Engineers, London 40(1):13-20. 1962.

17. Vreedenberg, H. A. Heat transfer between a fluidized bed and a horizontal tube. Chemical Engineering Science 9:52-60. 1958.

18. Vreedenberg, H. A. Heat transfer between a fluidized bed and a vertical tube. Chemical Engineering Science 11:274-284. 1960.

19. Wen, C. Y. and M. Leva. Fluidized bed heat transfer: a general correlation. A. I. Ch. E. Journal 2:482-488. 1956.

20. Wender, L. and G. T. Cooper. Heat transfer between fluidized solids beds and boundary surfaces--correlation of data. A. I. Ch. E. Journal 4:15-23. 1958.

21. Yagi, S., D. Kunii and N. Wakao. Radially effective thermal conductivities in packed beds. In: International Heat Transfer Conference, Boulder, Colorado and Westminster, Eng., 1961-62. International developments in heat transfer. vol. 4. New York, American Society of Mechanical Engineers, 1961-62. p. 742-749.

22. Yeh, George C. Generalized transfer factors for granular beds. Journal of Chemical and Engineering Data 6:526-530. 1961.

APPENDICES

APPENDIX A.

NOMENCLATURE

Symbol	Meaning	Units
A	cross-sectional area; A_w, area through which rate of heat transfer is q_w	ft^2
C	coefficient of discharge	
C	heat capacity; C_g heat capacity of solid; C_g heat capacity of gas	$Btu/lb._m {}^\circ F.$
D_p	Particle diameter	feet, inches
d	Diameter; d_o diameter of tube; d_e, equivalent diameter 4(free cross-sectional area) wetted perimeter	feet
G	mass velocity; G_e, geometric mean mass velocity	$lb._m/hr.ft^2$
g	acceleration of gravity	ft/sec^2
g	gravitational constant, 32.1740	$\frac{lb_m\ ft}{lb_f\ sec^2}$
h	local heat transfer coefficient	$Btu/hr.ft^2 {}^\circ F$
h	average heat transfer coefficient	$Btu/hr.ft^2 {}^\circ F$
k	thermal conductivity	$Btu/hr.ft^2 \frac{{}^\circ F}{ft}$
L	length of heating tube; L_f, fluidized bed height; L_s, static bed height	feet
P	static pressure; ΔP, pressure difference	lb_f/ft^2
q	volumetric flow rate through orifice	$ft^3/sec.$
q	rate of heat transfer	Btu/hr.
T	temperature; $T_{b_{loc}}$, local bulk temperature of fluid; T_w, temperature of wall	°F

Symbol	Meaning	Units
W	mass velocity through orifice	lb_m/hr
x	distance from entrance along heating tube	inches
Y	expansion factor	
	Greek Symbols	
β	ratio of orifice diameter to pipe diameter	
Δ	final value minus initial value; increase	
ϵ	fraction voids	
K	ratio of constant pressure heat capacity to constant volume heat capacity	
μ	viscosity; μ_b viscosity at temperature T_b; μ_μ, viscosity at temperature T_w	$\frac{lb_m}{ft\ hr}$
ρ	density; ρ_g density of gas; ρ_s density of solid ρ_b, density of fluidized bed	lb_m/ft^3

Dimensionless Groups

Nu	Nusselt number	hd/k
Pr	Prandtl number	$C_p \mu/k$
Re	Reynolds number	$\frac{de\ G}{\mu}$

APPENDIX B.

Appendix Table 1

		Distance*	Probe position	Tube wall temperature	Temperature Difference	Local heat transfer coefficient
Run Number	JE-1	1.5	1	127.8	39.0	8.49
Type of beads	None	3.5	2	149.5	60.6	5.47
Static bed height	--	5.5	3	163.0	73.6	4.50
Heating tube location	1	15.5	4	190.7	99.0	3.35
Mass flow rate	4210	33.5	5	216.5	123.7	2.68
Average air inlet temperature	90.5	41.5	6	223.9	131.3	2.52
Heat flux	331.3	43.5	7	224.6	131.9	2.51
		45.5	8	225.9	133.5	2.48
Run Number	JE-2		1	142.9	46.1	7.21
Type of beads	None		2	166.6	69.3	4.80
Static bed height	--		3	180.9	83.8	3.97
Heating tube location	1		4**	206.2	109.5	3.04
Mass flow rate	3610		5**	238.1	142.0	2.34
Average air inlet temperature	96.7		6	249.1	150.1	2.22
Heat flux	332.6		7	252.3	153.1	2.17
			8	253.8	154.4	2.15
Run Number	JE-3		1	154.3	56.1	6.02
Type of beads	None		2	185.2	86.3	3.91
Static bed height	--		3	205.7	104.9	3.22
Heating tube location	1		4	241.2	139.6	2.42
Mass flow rate	2400		5	280.9	178.0	1.90
Average air inlet temperature	97.2		6	297.5	193.8	1.74
Heat flux	337.8		7	300.4	196.3	1.72
			8	304.7	201.1	1.68
Run Number	JE-4		1	190.4	90.3	3.83
Type of beads	None		2	240.8	136.3	2.54
Static bed height	--		3	266.5	160.5	2.16
Heating tube location	1		4	316.9	208.4	1.66
Mass flow rate	760		5	365.0	251.5	1.38
Average air inlet temperature	104.8		6	372.2	258.5	1.34
Heat flux	346.1		7	379.0	260.5	1.33
			8	381.6	263.2	1.31

* Distance from entrance corresponding to probe position number, inches.

** 13.5 inches and 31.5 inches.

		Probe position	Tube wall temperature	Temperature Difference	Local heat transfer coefficient
Run Number	JE-5	1	125.6	34.8	9.48
Type of beads	None	2	146.5	53.4	6.18
Static bed height	--	3	157.3	64.6	5.11
Heating tube location	2	4	187.7	93.4	3.53
Mass flow rate	3970	5	213.4	119.8	2.75
Average air inlet temperature	92.2	6	222.8	128.9	2.56
Heat flux	329.8	7	223.2	129.1	2.55
		8	224.2	126.9	2.60
Run Number	JE-6	1	127.2	35.7	9.27
Type of beads	None	2	146.1	56.3	5.88
Static bed height	--	3	159.1	67.0	4.94
Heating tube location	2	4	189.3	97.2	3.40
Mass flow rate	3700	5	221.2	127.1	2.60
Average air inlet temperature	91.7	6	232.5	138.0	2.40
Heat flux	330.9	7	233.6	139.0	2.38
		8	235.5	140.2	2.36
Run Number	JE-7	1	146.1	47.8	7.02
Type of beads	None	2	174.7	73.7	4.55
Static bed height	--	3	190.0	88.9	3.78
Heating tube location	2	4	235.2	132.2	2.54
Mass flow rate	2295	5	281.5	177.0	1.90
Average air inlet temperature	101.4	6	301.3	196.2	1.77
Heat flux	335.7	7	306.1	201.3	1.67
		8	309.4	201.5	1.67
Run Number	JE-8	1	179.6	78.8	4.41
Type of beads	None	2	223.2	119.2	2.92
Static bed height	--	3	252.1	145.9	2.38
Heating tube location	2	4	318.4	208.5	1.67
Mass flow rate	693	5	368.2	252.5	1.38
Average air inlet temperature	104.4	6	379.0	262.5	1.33
Heat flux	347.9	7	381.0	264.7	1.31
		8	383.4	267.3	1.30
Run Number	JE-9	1	130.1	38.2	8.72
Type of beads	None	2	147.7	56.4	5.90
Static bed height	--	3	157.6	65.9	5.05
Heating tube location	4	4	187.5	96.6	3.45
Mass flow rate	3820	5	210.0	119.7	2.78
Average air inlet temperature	92.6	6	217.4	125.8	2.65
Heat flux	333.0	7	214.7	122.6	2.72
		8	214.7	121.5	2.74

		Probe position	Tube wall temperature	Temperature Difference	Local heat transfer coefficient
Run Number	JE-10	1	134.6	42.6	7.82
Type of beads	None	2	155.1	62.3	5.35
Static bed height	--	3	165.9	73.5	4.53
Heating tube location	4	4	197.1	104.7	3.18
Mass flow rate	3310	5	223.2	131.8	2.53
Average air inlet temperature	92.9	6	231.4	138.7	2.40
Heat flux	333.0	7	229.8	137.0	2.43
		8	228.4	134.5	2.48
Run Number	JE-11	1	130.2	50.2	6.70
Type of beads	None	2	156.7	74.6	4.50
Static bed height	--	3	173.0	88.4	3.80
Heating tube location	4	4	209.5	124.0	2.71
Mass flow rate	2340	5	248.0	159.3	2.11
Average air inlet temperature	83.0	6	258.0	168.5	1.99
Heat flux	336.0	7	256.2	165.8	2.03
		8	252.5	161.5	2.08
Run Number	JE-12	1	172.7	81.1	4.19
Type of beads	None	2	203.8	110.8	3.10
Static bed height	--	3	226.5	130.1	2.64
Heating tube location	4	4	279.0	182.4	1.88
Mass flow rate	820	5	322.2	217.7	1.59
Average air inlet temperature	92.5	6	338.5	235.8	1.46
Heat flux	343.1	7	341.7	237.0	1.45
		8	339.3	235.0	1.46
Run Number	JE-13	1	112.2	32.9	10.1
Type of beads	None	2	127.8	49.3	6.75
Static bed height	--	3	141.8	61.2	5.43
Heating tube location	3	4	171.3	89.8	3.70
Mass flow rate	3740	5	192.3	109.1	3.05
Average air inlet temperature	80.5	6	197.2	113.5	2.93
Heat flux	332.6	7	197.5	113.7	2.93
		8	197.7	113.6	2.93
Run Number	JE-14	1	122.3	36.2	9.21
Type of beads	None	2	144.2	55.5	6.01
Static bed height	--	3	155.7	69.4	4.80
Heating tube location	3	4	190.0	101.6	3.28
Mass flow rate	3040	5	214.8	126.0	2.65
Average air inlet temperature	86.0	6	220.3	129.9	2.57
Heat flux	333.3	7	221.0	130.7	2.55
		8	221.8	131.4	2.54

		Probe position	Tube wall temperature	Temperature Difference	Local heat transfer coefficient
Run Number	JE-15	1	131.3	41.5	8.01
Type of beads	None	2	153.3	65.6	5.07
Static bed height	--	3	166.0	79.9	4.16
Heating tube location	3	4	208.2	120.0	2.77
Mass flow rate	2340	5	237.3	146.8	2.27
Average air inlet temperature	88.0	6	245.0	154.1	2.16
Heat flux	332.6	7	245.7	154.2	2.16
		8	245.7	154.0	2.16
Run Number	JE-16	1	155.3	65.2	5.16
Type of beads	None	2	139.5	97.6	3.45
Static bed height	--	3	208.0	116.9	2.88
Heating tube location	3	4	267.5	173.1	1.94
Mass flow rate	930	5	312.5	215.0	1.57
Average air inlet temperature	90.0	6	321.0	222.5	1.51
Heat flux	336.5	7	322.2	222.4	1.51
		8	320.2	220.0	1.53

		Distance*	Probe position	Tube wall temperature	Temperature Difference	Local heat transfer coefficient	Bed Density
Run Number	AA-1	1.5	1	100.7	15.2	21.8	
Type of beads	Coarse	3.5	2	108.7	21.8	15.2	
Static bed height	3	5.5	3	113.5	26.7	12.4	6.6
Heating tube location	3	11.5	4	118.7	31.2	10.6	
		17.5	5	137.2	48.9	6.77	
Mass flow rate	2730	23.5	6	171.5	84.0	3.94	1.4
Average air inlet temperature	86.7	29.5	7	217.8	128.8	2.57	
		35.5	8	238.8	149.8	2.21	
Heat flux	330.9	41.5	9	244.7	154.1	2.15	0.5
		43.5	10	245.3	155.0	2.13	
		45.5	11	241.5	150.0	2.21	
Run Number	AA-2		1	100.0	12.9	25.8	
Type of beads	Coarse		2	106.5	19.3	17.3	
Static bed height	3		3	110.5	22.9	14.5	5.0
Heating tube location	3		4	121.2	33.1	10.0	
			5	165.0	77.3	4.31	
Mass flow rate	2240		6	205.2	117.4	2.84	0.2
Average air inlet temperature	86.7		7	225.8	137.0	2.43	
			8	232.8	143.6	2.32	
Heat flux	333.0		9	236.0	146.0	2.28	0.2
			10	236.0	145.9	2.28	
			11	235.3	146.1	2.28	
Run Number	AA-3		1	95.7	10.5	30.8	
Type of beads	Coarse		2	96.3	11.1	29.2	
Static bed height	9		3	95.7	10.4	31.1	23.4
Heating tube location	3		4	104.0	17.3	18.7	
			5	109.7	23.0	14.1	
Mass flow rate	2295		6	112.2	24.8	13.0	9.5
Average air inlet temperature	85.3		7	118.7	32.3	10.0	
			8	153.0	65.4	4.95	
Heat flux	323.6		9	198.3	112.9	2.87	5.0
			10	204.7	118.8	2.72	
			11	210.8	123.1	2.63	
Run Number	AA-4		1	93.8	11.7	27.9	
Type of beads	Coarse		2	94.8	12.0	27.2	
Static bed height	9		3	93.8	11.1	29.4	20.9
Heating tube location	3		4	105.3	21.9	14.9	
			5	107.5	24.1	13.5	
Mass flow rate	2510		6	109.8	25.5	12.8	10.0
Average air inlet temperature	82.4		7	112.2	27.7	11.8	
			8	120.2	34.4	9.53	
Heat flux	326.0		9	145.7	59.8	5.45	6.6
			10	155.3	70.0	4.66	
			11	174.0	90.1	3.62	

		Probe position	Tube wall temperature	Temperature Difference	Local heat transfer coefficient	Bed Density
Run Number	AA-5	1	94.7	11.1	29.6	
Type of beads	Coarse	2	97.7	11.8	27.8	
Static bed height	9	3	98.0	8.1	40.5	15.9
Heating tube		4	101.0	11.5	28.5	
location	3	5	119.7	31.4	10.4	
Mass flow rate	1610	6	168.0	78.8	4.16	0.94
Average air inlet		7	196.8	107.8	3.04	
temperature	87.3	8	215.2	108.4	3.03	
Heat flux	328.1	9	227.3	134.2	2.45	0.47
		10	229.7	137.2	2.39	
		11	234.3	140.1	2.34	
Run Number	AA-6	1	93.7	11.7	28.6	
Type of beads	Coarse	2	95.5	11.5	29.1	
Static bed height	15	3	96.7	10.8	31.0	46.8
Heating tube		4	95.7	10.1	33.1	
location	3	5	95.0	10.0	33.4	
Mass flow rate	1960	6	107.7	21.5	15.5	11.9
Average air inlet		7	111.5	25.4	13.2	
temperature	83.3	8	126.3	40.2	8.3	
Heat flux	334.3	9	167.5	79.6	4.20	5.62
		10	178.5	91.3	3.66	
		11	192.0	106.4	3.14	
Run Number	AA-7	1	97.5	16.8	19.6	
Type of beads	Coarse	2	109.7	28.1	11.7	
Static bed height	15	3	116.5	33.3	9.88	54.4
Heating tube		4	123.7	38.3	8.48	
location	3	5	129.7	43.7	7.53	
Mass flow rate	1450	6	134.3	47.9	6.87	18.4
Average air inlet		7	138.5	52.0	6.33	
temperature	82.0	8	142.7	56.2	5.86	
Heat flux	329.1	9	149.2	62.2	5.29	0.2
		10	151.2	64.8	5.08	
		11	158.5	72.7	4.53	
Run Number	AA-8	1	159.8	66.8	4.97	
Type of beads	Coarse	2	157.3	68.0	4.89	
Static bed height	15	3	139.7	49.0	6.78	57.9
Heating tube		4	125.7	23.3	14.3	
location	3	5	100.7	6.80	48.9	
Mass flow rate	818	6	157.3	63.3	5.25	8.6
Average air inlet		7	199.0	105.4	3.15	
temperature	90.0	8	226.7	128.8	2.59	
Heat flux	332.3	9	244.5	145.6	2.28	0.2
		10	249.7	150.0	2.22	
		11	252.2	153.1	2.18	

		Probe position	Tube wall temperature	Temperature difference	Local heat transfer coefficient	Bed Density
Run Number	AA-9	1	97.5	16.9	19.5	
Type of beads	Coarse	2	109.7	27.5	12.0	
Static bed height	3	3	116.5	32.8	10.0	5.1
Heating tube		4	123.7	39.5	8.22	
location	1	5	129.7	44.7	7.36	
Mass flow rate	2800	6	134.3	49.2	6.69	3.0
Average air inlet		7	138.5	53.7	6.13	
temperature	82.0	8	142.7	58.3	5.64	0.94
Heat flux	329.1	9	149.7	64.6	5.09	
		10	151.2	67.4	4.88	
		11	158.5	75.3	4.37	
Run Number	AA-10	1	96.5	11.9	27.8	
Type of beads	Coarse	2	106.8	21.6	15.3	
Static bed height	3	3	108.5	23.7	14.0	4.1
Heating tube		4	127.3	42.3	7.83	
location	1	5	173.7	90.0	3.68	
Mass flow rate	2213	6	206.0	123.6	2.68	
Average air inlet		7	222.7	137.0	2.42	
temperature	83.8	8	233.2	147.0	2.25	
Heat flux	331.3	9	242.7	156.6	2.12	0.2
		10	246.0	159.7	2.07	
		11	250.3	164.6	2.01	
Run Number	AB-1	1	92.8	11.5	28.6	
Type of beads	Coarse	2	97.3	14.2	23.2	
Static bed height	9	3	99.8	15.6	21.1	19.3
Heating tube		4	108.5	23.5	14.0	
location	1	5	108.7	22.8	14.4	
Mass flow rate	2520	6	113.5	26.9	12.2	6.4
Average air inlet		7	135.0	46.5	7.08	
temperature	84.3	8	179.3	90.9	3.62	
Heat flux	329.4	9	207.0	117.1	2.81	5.5
		10	219.0	129.8	2.54	
		11	225.0	134.8	2.44	
Run Number	AB-2	1	98.2	11.9	27.9	
Type of beads	Coarse	2	101.3	13.9	23.9	
Static bed height	9	3	103.0	14.5	22.9	28.4
Heating tube		4	101.5	14.7	22.6	
location	1	5	105.3	18.8	17.7	
Mass flow rate	2290	6	127.3	40.2	8.26	3.4
Average air inlet		7	159.5	74.2	4.47	
temperature	84.3	8	193.7	109.3	3.04	
Heat flux	331.9	9	216.2	129.6	2.56	0.47
		10	219.8	133.2	2.49	
		11	225.5	139.2	2.38	

		Probe position	Tube wall temperature	Temperature difference	Local heat transfer coefficient	Bed Density
Run Number	AB-3	1	95.5	10.7	30.5	
Type of beads	Coarse	2	96.0	10.9	30.0	
Static bed height	9	3	97.7	11.6	28.2	31.5
Heating tube		4	98.0	10.5	31.1	
location	1	5	126.7	39.5	8.27	
Mass flow rate	1575	6	175.8	88.6	3.69	1.9
Average air inlet		7	198.5	111.9	2.92	
temperature	85.4	8	200.7	127.1	2.57	
Heat flux	326.7	9	233.2	142.1	2.30	0.2
		10	241.0	156.6	2.09	
		11	248.0	156.6	2.09	
Run Number	AB-4	1	96.0	11.8	27.3	
Type of beads	Coarse	2	96.7	11.7	27.6	
Static bed height	15	3	97.3	11.2	28.8	47.6
Heating tube		4	99.2	12.3	26.2	
location	1	5	98.5	9.86	32.7	
Mass flow rate	535	6	102.2	12.4	26.0	16.8
Average air inlet		7	129.0	36.3	8.88	
temperature	81.8	8	158.0	66.5	4.85	
Heat flux	322.5	9	182.8	90.7	3.56	1.6
		10	191.7	99.9	3.23	
		11	199.8	108.1	2.98	
Run Number	AB-5	1	89.3	11.6	28.1	
Type of beads	Coarse	2	90.8	11.8	27.7	
Static bed height	15	3	91.0	11.0	29.7	42.0
Heating tube		4	94.2	13.6	24.0	
location	1	5	94.2	12.9	25.3	
Mass flow rate	1480	6	108.3	26.9	12.1	15.6
Average air inlet		7	145.5	61.0	5.35	
temperature	79.2	8	174.2	92.1	3.54	
Heat flux	326.4	9	197.2	114.7	2.85	0.2
		10	204.5	119.3	2.74	
		11	211.8	126.2	2.58	
Run Number	AB-6	1	93.7	12.4	25.7	
Type of beads	Coarse	2	94.0	11.1	28.7	
Static bed height	15	3	94.0	9.3	34.3	49.0
Heating tube		4	94.0	7.9	40.4	
location	1	5	102.2	15.0	21.3	
Mass flow rate	877	6	154.8	64.1	4.98	8.1
Average air inlet		7	196.8	106.3	3.0	
temperature	84.5	8	221.5	128.6	2.48	
Heat flux	319.0	9	241.7	148.4	2.15	0.2
		10	254.3	160.7	1.99	
		11	261.8	167.9	1.90	

		Probe position	Tube wall temperature	Temperature difference	Local heat transfer coefficient	Bed Density
Run Number	AB-7	1	89.0	13.8	23.98	
Type of beads	Coarse	2	94.2	17.2	19.2	
Static bed height	3	3	94.2	17.0	19.5	2.70
Heating tube		4	126.3	49.8	6.64	
location	2	5	169.3	91.7	3.61	
Mass flow rate	2250	6	197.7	120.7	2.74	0.47
Average air inlet		7	212.8	135.9	2.43	
temperature	76.9	8	225.0	144.6	2.29	
Heat flux	330.9	9	236.0	155.2	2.13	0.20
		10	239.8	158.6	2.09	
		11	243.3	162.0	2.04	
Run Number	AB-8	1	86.0	14.8	22.1	
Type of beads	Coarse	2	93.7	19.4	16.9	
Static bed height	3	3	94.7	19.3	17.0	5.50
Heating tube		4	110.2	34.4	9.52	
location	2	5	136.3	59.4	5.51	
Mass flow rate	2800	6	139.5	62.7	5.22	1.90
Average air inlet		7	178.8	100.4	3.26	
temperature	75.7	8	209.2	112.4	2.91	
Heat flux	327.4	9	225.8	144.6	2.26	0.63
		10	234.2	144.1	2.27	
		11	238.8	159.1	2.06	
Run Number	AB-9	1	89.5	12.2	26.5	
Type of beads	Coarse	2	93.0	13.9	23.3	
Static bed height	9	3	95.2	15.4	21.0	26.7
Heating tube		4	95.7	15.7	20.6	
location	2	5	101.7	20.8	15.5	
Mass flow rate	2570	6	113.7	31.3	10.3	6.40
Average air inlet		7	146.8	61.2	5.28	
temperature	80.0	8	169.8	85.3	3.79	
Heat flux	323.2	9	197.8	115.3	2.80	0.20
		10	219.0	133.2	2.43	
		11	223.0	138.8	2.34	
Run Number	AB-10	1	89.3	11.4	28.5	
Type of beads	Coarse	2	94.3	14.1	23.0	
Static bed height	9	3	95.3	15.2	21.4	20.4
Heating tube		4	94.8	14.2	22.9	
location	2	5	101.7	22.0	14.8	
Mass flow rate	2250	6	122.8	42.5	7.63	
Average air inlet		7	159.0	80.1	4.05	
temperature	77.7	8	188.8	110.8	2.93	
Heat flux	324.6	9	209.0	127.8	2.54	0.20
		10	213.7	132.7	2.45	
		11	217.0	136.1	2.39	

		Probe position	Tube wall temperature	Temperature difference	Local heat transfer coefficient	Bed Density
Run Number	AB-11	1	92.5	12.6	25.6	
Type of beads	Coarse	2	95.2	15.2	21.2	
Static bed height	9	3	95.3	14.7	22.0	31.5
Heating tube		4	90.3	10.9	29.6	
location	2	5	130.0	48.3	6.67	
Mass flow rate	1540	6	177.2	96.7	3.55	0.47
Average air inlet		7	195.7	115.3	2.79	
temperature	80.4	8	215.8	131.1	2.46	
Heat flux	322.2	9	234.0	149.0	2.16	0.20
		10	240.3	154.3	2.09	
		11	245.3	160.1	2.01	
Run Number	AB-12	1	90.3	13.6	23.6	
Type of beads	Coarse	2	91.7	13.6	23.6	
Static bed height	15	3	93.5	15.1	21.3	48.7
Heating tube		4	91.7	13.2	24.4	
location	2	5	91.3	11.7	27.5	
Mass flow rate	2020	6	95.0	15.2	21.2	25.1
Average air inlet		7	111.3	30.4	10.6	
temperature	77.7	8	148.3	68.5	4.69	
Heat flux	321.5	9	184.3	103.4	3.11	
		10	191.5	111.6	2.88	2.30
		11	201.5	121.3	2.65	
Run Number	AB-13	1	85.3	9.0	36.1	
Type of beads	Coarse	2	90.8	10.9	29.8	
Static bed height	15	3	93.5	12.3	26.4	52.9
Heating tube		4	95.2	12.1	26.8	
location	2	5	96.8	11.1	29.2	
Mass flow rate	1415	6	113.2	25.8	12.6	16.8
Average air inlet		7	160.0	74.1	4.38	
temperature	81.3	8	189.3	102.5	3.17	
Heat flux	324.6	9	210.0	124.3	2.61	0.20
		10	216.0	126.9	2.56	
		11	225.2	135.2	2.40	
Run Number	AB-14	1	97.5	11.2	28.9	
Type of beads	Coarse	2	98.3	11.1	29.1	
Static bed height	15	3	99.7	11.5	28.1	54.6
Heating tube		4	100.8	10.8	29.9	
location	2	5	113.2	21.0	15.4	
Mass flow rate	820	6	140.3	49.2	6.57	12.0
Average air inlet		7	184.3	102.2	3.16	
temperature	87.2	8	226.3	131.6	2.46	
Heat flux	323.2	9	255.2	160.3	2.02	0.20
		10	268.0	171.6	1.88	
		11	276.3	179.8	1.80	

		Probe position	Tube wall temperature	Temperature difference	Local heat transfer coefficient	Bed Density
Run Number	AB-15	1	92.5	15.9	20.7	
Type of beads	Coarse	2	99.7	20.9	15.7	
Static bed height	3	3	102.0	23.2	14.2	5.10
Heating tube		4	114.3	35.1	9.35	
location	4	5	130.0	50.4	6.52	
Mass flow rate	2850	6	150.3	71.4	4.60	1.90
Average air inlet		7	178.3	100.4	3.27	
temperature	78.0	8	203.3	122.6	2.68	
Heat flux	328.4	9	229.8	149.5	2.20	0.20
		10	232.2	150.9	2.20	
		11	231.3	149.8	2.20	
Run Number	AB-15 A	1	91.5	14.0	23.6	
Type of beads	Coarse	2	96.3	11.5	28.8	
Static bed height	3	3	97.8	19.2	17.2	3.40
Heating tube		4	119.5	40.0	8.27	
location	4	5	168.0	89.1	3.71	
Mass flow rate	2290	6	200.2	121.8	2.72	0.20
Average air inlet		7	213.2	134.5	2.46	
temperature	78.8	8	220.8	138.6	2.39	
Heat flux	330.9	9	226.8	144.5	2.29	0.20
		10	229.5	146.7	2.26	
		11	229.5	146.5	2.26	
Run Number	AB-16	1	89.7	11.7	27.5	
Type of beads	Coarse	2	91.2	12.5	25.7	
Static bed height	9	3	91.5	13.1	24.6	29.2
Heating tube		4	95.0	15.3	21.0	
location	4	5	101.7	21.8	14.8	
Mass flow rate	2590	6	115.8	34.5	9.30	4.06
Average air inlet		7	138.7	57.6	5.59	
temperature	79.1	8	167.5	86.0	3.74	
Heat flux	321.8	9	192.3	111.0	2.93	1.40
		10	198.3	117.9	2.73	
		11	204.7	123.5	2.61	
Run Number	AB-17	1	93.8	10.7	30.1	
Type of beads	Coarse	2	94.0	10.8	29.8	
Static bed height	9	3	94.8	11.6	27.7	30.6
Heating tube		4	96.5	13.0	24.8	
location	4	5	107.0	22.0	14.6	
Mass flow rate	2240	6	131.5	46.3	6.95	5.00
Average air inlet		7	169.7	85.9	3.75	
temperature	82.9	8	194.7	112.7	2.86	
Heat flux	321.8	9	211.2	124.5	2.58	0.20
		10	215.2	128.4	2.51	
		11	216.8	129.8	2.98	

		Probe position	Tube wall temperature	Temperature difference	Local heat transfer coefficient	Bed density
Run Number	AB-18	1	93.5	9.0	36.6	
Type of beads	Coarse	2	97.2	10.2	32.3	
Static bed height	9	3	97.7	11.2	29.4	28.5
Heating tube		4	100.7	14.0	23.5	
location	4	5	134.3	47.8	6.89	
Mass flow rate	1580	6	183.2	96.9	3.40	
Average air inlet		7	202.5	116.4	2.83	
temperature	85.0	8	216.0	127.0	2.59	
Heat flux	329.4	9	229.5	140.0	2.35	
		10	233.0	143.4	2.30	
		11	236.2	145.9	2.26	
Run Number	AB-19	1	94.7	11.4	28.1	
Type of beads	Coarse	2	97.0	13.6	23.6	
Static bed height	15	3	95.5	12.5	25.6	48.5
Heating tube		4	96.2	11.7	27.4	
location	4	5	97.0	12.7	25.2	
Mass flow rate	2030	6	101.2	16.1	19.9	
Average air inlet		7	118.5	33.6	9.54	
temperature	82.6	8	157.2	72.0	4.45	
Heat flux	320.5	9	188.7	104.3	3.07	4.10
		10	195.8	111.0	2.89	
		11	200.3	113.2	2.83	
Run Number	AB-19 A	1	93.8	11.8	27.7	
Type of beads	Coarse	2	94.0	12.3	26.6	
Static bed height	15	3	95.0	12.3	26.6	53.0
Heating tube		4	95.7	12.8	25.6	
location	4	5	95.7	12.1	27.0	
Mass flow rate	1450	6	109.2	24.4	13.4	15.6
Average air inlet		7	156.2	71.7	4.56	
temperature	82.3	8	186.8	102.8	3.18	
Heat flux	327.2	9	202.5	116.0	2.82	0.20
		10	210.0	122.5	2.67	
		11	214.3	125.7	2.60	
Run Number	AB-20	1	107.2	22.7	14.4	
Type of beads	Coarse	2	99.7	15.1	21.6	
Static bed height	15	3	98.7	13.3	24.6	55.5
Heating tube		4	96.5	9.2	35.5	
location	4	5	97.5	8.7	37.5	
Mass flow rate	876	6	153.2	64.6	5.05	
Average air inlet		7	202.3	111.3	2.93	
temperature	83.3	8	225.5	134.5	2.43	
Heat flux	326.2	9	243.3	152.1	2.14	0.20
		10	247.3	158.4	2.06	
		11	248.0	158.4	2.06	

		Probe position	Tube wall temperature	Temperature difference	Local heat transfer coefficient	Bed density
Run Number	AB-21	1	90.2	8.0	40.2	
Type of beads	Fine	2	97.0	13.5	23.8	
Static bed height	3	3	98.3	14.7	21.9	4.40
Heating tube		4	103.8	19.0	16.9	
location	4	5	106.5	20.3	15.8	
Mass flow rate	1070	6	107.7	20.4	15.8	3.00
Average air inlet		7	109.7	20.8	15.5	
temperature	82.9	8	110.5	20.7	15.5	
Heat flux	321.5	9	111.8	21.1	15.2	2.70
		10	106.5	15.6	20.6	
		11	115.3	24.0	13.4	
Run Number	AB-22	1	90.3	6.0	53.9	
Type of beads	Fine	2	92.2	6.8	47.5	
Static bed height	3	3	94.2	8.3	38.9	3.00
Heating tube		4	109.2	21.4	15.1	
location	4	5	120.5	30.9	10.5	
Mass flow rate	817	6	128.7	37.4	8.64	1.60
Average air inlet		7	135.5	43.2	7.48	
temperature	85.5	8	141.3	47.2	6.85	
Heat flux	323.2	9	145.3	50.3	6.43	0.62
		10	144.0	48.7	6.64	
		11	161.0	65.6	4.93	
Run Number	X-1	1	78.5	2.72	118.1	
Type of beads	Fine	2	---	---	---	
Static bed height	6	3	86.0	6.97	46.1	15.3
Heating tube		4	93.0	11.3	28.6	
location	4	5	99.5	16.4	19.6	
Mass flow rate	1110	6	102.5	18.3	17.5	6.40
Average air inlet		7	105.7	19.1	16.8	
temperature	78.2	8	107.7	20.6	15.6	
Heat flux	321.2	9	108.6	19.9	16.1	
		10	105.7	17.0	18.9	
		11	---	---	---	
Run Number	X-2	1	90.2	5.77	55.3	
Type of beads	Fine	2	---	---	---	
Static bed height	6	3	91.0	5.63	56.7	14.8
Heating tube		4	97.8	13.8	23.1	
location	4	5	110.8	23.3	13.7	
Mass flow rate	817	6	119.0	29.4	10.9	1.50
Average air inlet		7	124.7	34.1	9.35	
temperature	83.7	8	130.0	38.5	8.29	
Heat flux	319.0	9	135.7	43.4	7.35	0.62
		10	134.8	41.2	7.74	
		11	---	---	---	

		Probe position	Tube wall temperature	Temperature difference	Local heat transfer coefficient	Bed density
Run Number	AB-23	1	92.8	6.2	51.2	
Type of beads	Fine	2	93.2	6.3	50.4	
Static bed height	9	3	93.7	6.2	51.2	24.2
Heating tube		4	96.7	8.3	38.3	
location	4	5	98.7	9.7	32.7	
Mass flow rate	1070	6	104.5	14.0	22.7	5.60
Average air inlet		7	109.2	17.9	17.7	
temperature	86.2	8	111.8	19.9	16.0	
Heat flux	317.6	9	115.5	22.1	14.4	4.40
		10	110.2	16.5	19.2	
		11	122.0	27.4	11.6	
Run Number	AB-24	1	84.7	3.9	83.8	
Type of beads	Fine	2	87.3	3.9	83.8	
Static bed height	9	3	88.7	3.3	99.0	31.5
Heating tube		4	90.2	3.13	95.9	
location	4	5	101.8	13.2	40.4	
Mass flow rate	616	6	122.8	31.1	9.52	1.60
Average air inlet		7	145.7	53.3	6.14	
temperature	82.5	8	165.2	71.8	4.55	
Heat flux	326.4	9	177.8	82.8	3.94	0.20
		10	180.3	84.9	3.85	
		11	194.2	99.6	3.28	
Run Number	AC-1	1	85.5	6.3	51.3	
Type of beads	Fine	2	86.3	6.4	50.5	
Static bed height	15	3	86.5	5.9	54.8	51.5
Heating tube		4	86.0	5.8	55.8	
location	4	5	86.7	3.9	82.9	
Mass flow rate	817	6	89.8	7.4	43.7	22.6
Average air inlet		7	105.5	18.5	17.5	
temperature	79.6	8	133.0	44.7	7.24	
Heat flux	323.5	9	169.8	81.7	3.96	3.10
		10	177.8	87.9	3.68	
		11	194.5	105.4	3.07	
Run Number	AC-2	1	88.2	7.6	41.3	
Type of beads	Fine	2	88.7	8.4	37.4	
Static bed height	15	3	89.5	8.2	38.3	39.0
Heating tube		4	89.3	7.0	44.9	
location	4	5	89.7	7.1	44.3	
Mass flow rate	1110	6	93.2	9.0	34.9	24.2
Average air inlet		7	94.2	10.4	30.2	
temperature	79.5	8	97.3	12.1	26.0	
Heat flux	314.2	9	104.8	18.7	16.8	
		10	103.8	16.0	19.6	
		11	119.0	32.5	9.67	

		Probe position	Tube wall temperature	Temperature difference	Local heat transfer coefficient	Bed density
Run Number	AC-3	1	92.0	12.3	26.0	
Type of beads	Fine	2	99.8	19.1	16.7	
Static bed height	3	3	102.2	19.8	16.1	4.80
Heating tube		4	104.3	20.9	15.3	
location	1	5	106.0	21.7	14.7	
Mass flow rate	1200	6	107.7	22.5	14.2	3.60
Average air inlet		7	108.5	22.3	14.3	
temperature	80.4	8	108.3	21.2	15.0	
Heat flux	319.5	9	102.2	14.7	21.7	3.60
		10	102.3	14.9	21.4	
		11	109.3	21.4	14.9	
Run Number	AC-4	1	88.5	6.5	50.4	
Type of beads	Fine	2	89.0	5.9	55.5	
Static bed height	3	3	90.7	6.4	51.2	4.80
Heating tube		4	107.0	21.0	15.6	
location	1	5	116.8	29.7	11.0	
Mass flow rate	817	6	123.7	34.4	9.52	
Average air inlet		7	128.8	29.0	8.39	
temperature	82.8	8	131.5	40.9	8.00	
Heat flux	327.4	9	133.8	41.8	7.83	1.10
		10	139.8	46.8	7.00	
		11	149.3	57.0	5.74	
Run Number	AC-5	1	91.3	8.5	37.1	
Type of beads	Fine	2	91.5	8.5	37.1	
Static bed height	6	3	91.5	7.9	39.9	13.9
Heating tube		4	95.3	10.5	30.0	
location	1	5	100.3	15.2	20.7	
Mass flow rate	1155	6	103.8	17.0	18.5	6.90
Average air inlet		7	106.0	18.7	16.9	
temperature	82.7	8	108.3	19.1	16.5	
Heat flux	315.3	9	103.5	13.6	23.2	5.50
		10	104.8	14.8	21.3	
		11	113.0	22.6	14.0	
Run Number	AC-7	1	90.5	7.3	43.2	
Type of beads	Fine	2	91.8	8.5	37.1	
Static bed height	9	3	93.5	9.8	32.2	23.4
Heating tube		4	93.3	8.5	37.1	
location	1	5	94.5	8.6	36.7	
Mass flow rate	1190	6	99.7	13.4	23.5	10.5
Average air inlet		7	104.3	16.2	19.5	
temperature	82.8	8	106.5	18.0	17.5	
Heat flux	315.3	9	103.0	13.0	24.3	7.50
		10	103.8	13.7	23.0	
		11	112.0	22.0	14.3	

		Probe position	Tube wall temperature	Temperature difference	Local heat transfer coefficient	Bed density
Run Number	AC-6	1	84.7	4.6	69.5	
Type of beads	Fine	2	85.3	4.9	65.2	
Static bed height	6	3	88.7	6.4	49.9	17.5
Heating tube		4	90.8	6.6	48.4	
location	1	5	106.8	19.6	16.3	
Mass flow rate	817	6	117.2	28.5	11.2	2.30
Average air inlet		7	124.0	34.7	9.21	
temperature	80.4	8	129.7	39.1	8.17	
Heat flux	319.5	9	134.3	42.8	7.46	1.10
		10	139.5	47.3	6.75	
		11	151.2	59.2	5.40	
Run Number	AC-8	1	90.7	6.7	47.6	
Type of beads	Fine	2	91.2	5.6	56.9	
Static bed height	9	3	91.7	6.0	53.1	34.5
Heating tube		4	92.5	5.8	54.9	
location	1	5	97.8	10.2	31.2	
Mass flow rate	817	6	125.0	37.0	8.61	4.40
Average air inlet		7	148.3	59.5	5.36	
temperature	83.7	8	168.5	79.4	4.01	
Heat flux	318.7	9	184.7	94.3	3.38	0.47
		10	140.3	100.1	3.18	
		11	205.7	115.2	2.77	
Run Number	AC-9	1	80.8	4.3	74.3	
Type of beads	Fine	2	85.7	6.3	50.7	
Static bed height	15	3	87.7	6.8	47.0	44.1
Heating tube		4	89.0	7.3	43.8	
location	1	5	91.0	7.1	45.0	
Mass flow rate	1150	6	92.2	9.3	34.4	29.5
Average air inlet		7	94.8	10.0	32.0	
temperature	78.8	8	107.2	20.9	15.3	
Heat flux	319.5	9	114.5	27.7	11.5	9.40
		10	123.3	36.7	8.71	
		11	134.0	47.2	6.77	
Run Number	AC-10	1	92.0	5.1	62.8	
Type of beads	Fine	2	92.3	5.0	64.1	
Static bed height	15	3	93.7	5.4	59.3	54.9
Heating tube		4	95.3	6.1	52.5	
location	1	5	95.3	5.0	64.1	
Mass flow rate	817	6	96.5	5.0	64.1	26.7
Average air inlet		7	110.8	17.6	18.2	
temperature	85.9	8	136.2	42.5	7.54	
Heat flux	320.5	9	165.5	71.7	4.47	2.30
		10	176.0	81.4	3.94	
		11	198.0	104.4	3.07	

		Probe position	Tube wall temperature	Temperature difference	Local heat transfer coefficient	Bed density
Run Number	AC-11	1	90.7	8.5	37.8	
Type of beads	Fine	2	96.7	13.4	24.0	
Static bed height	3	3	99.5	15.9	20.2	6.10
Heating tube		4	103.7	18.3	17.6	
location	1	5	106.8	20.8	15.5	
Mass flow rate	1110	6	109.0	21.7	14.8	4.80
Average air inlet		7	111.0	22.8	14.1	
temperature	82.3	8	112.0	22.9	14.0	
Heat flux	321.5	9	111.0	20.6	15.6	4.40
		10	107.5	16.8	19.1	
		11	112.0	23.6	13.6	
Run Number	AC-12	1	88.0	6.6	48.7	
Type of beads	Fine	2	89.0	6.8	47.2	
Static bed height	3	3	92.0	8.4	38.2	4.80
Heating tube		4	102.8	18.1	17.7	
location	2	5	112.0	24.0	13.4	
Mass flow rate	860	6	116.8	27.3	11.8	1.90
Average air inlet		7	120.3	29.4	10.9	
temperature	83.1	8	123.0	30.9	10.4	
Heat flux	321.2	9	124.8	31.4	10.2	1.60
		10	123.2	29.6	10.9	
		11	135.7	43.6	7.37	
Run Number	AC-13	1	91.8	7.6	41.5	
Type of beads	Fine	2	93.5	8.5	37.1	
Static bed height	6	3	94.3	8.2	38.5	12.0
Heating tube		4	96.7	10.6	29.7	
location	2	5	102.3	14.9	21.2	
Mass flow rate	1195	6	105.8	17.6	17.9	
Average air inlet		7	108.3	19.6	16.1	6.60
temperature	83.9	8	110.2	21.0	15.0	
Heat flux	315.3	9	110.2	19.9	15.8	5.60
		10	108.3	17.5	18.0	
		11	115.0	24.5	12.9	
Run Number	AC-14	1	87.3	4.7	68.5	
Type of beads	Fine	2	89.3	5.2	61.9	
Static bed height	6	3	91.5	6.3	51.0	27.6
Heating tube		4	94.0	7.0	46.0	
location	2	5	105.3	16.9	19.0	
Mass flow rate	817	6	115.7	25.4	12.7	2.30
Average air inlet		7	122.7	31.3	10.3	
temperature	83.4	8	127.5	35.6	9.04	
Heat flux	321.8	9	130.3	37.3	8.63	1.10
		10	132.8	38.8	8.30	
		11	145.5	52.4	6.14	

		Probe position	Tube wall temperature	Temperature difference	Local heat transfer coefficient	Bed density
Run Number	AC-15	1	90.7	6.9	45.7	
Type of beads	Fine	2	91.7	8.2	38.5	
Static bed height	9	3	92.5	8.6	36.7	21.1
Heating tube		4	92.8	8.6	36.7	
location	1	5	94.0	8.4	37.5	
Mass flow rate	1170	6	98.8	14.0	22.5	8.10
Average air inlet		7	103.2	16.1	19.6	
temperature	82.3	8	106.2	17.2	18.3	
Heat flux	315.3	9	105.7	16.9	18.7	5.10
		10	103.5	14.7	21.4	
		11	110.3	22.0	14.3	
Run Number	AC-16	1	90.0	5.2	61.3	
Type of beads	Fine	2	90.3	5.4	59.1	
Static bed height	9	3	90.8	5.3	60.2	34.5
Heating tube		4	92.7	5.5	58.0	
location	2	5	94.7	6.5	49.1	
Mass flow rate	693	6	113.3	23.4	13.6	2.70
Average air inlet		7	127.3	37.1	8.60	
temperature	83.4	8	139.3	47.9	6.66	
Heat flux	319.0	9	149.5	56.5	5.65	0.94
		10	152.5	57.8	5.52	
		11	166.8	72.2	4.41	
Run Number	AC-17	1	87.2	7.6	42.0	
Type of beads	Fine	2	87.8	7.8	41.0	
Static bed height	15	3	88.5	7.9	40.4	48.5
Heating tube		4	89.3	7.7	41.4	
location	2	5	89.8	7.4	43.2	
Mass flow rate	1110	6	91.7	8.0	39.9	30.1
Average air inlet		7	93.3	8.9	35.8	
temperature	79.5	8	106.0	19.8	16.1	
Heat flux	319.5	9	115.2	28.4	11.3	7.20
		10	116.8	29.8	10.7	
		11	134.0	47.2	6.77	
Run Number	AC-18	1	83.0	3.2	101.0	
Type of beads	Fine	2	84.3	3.6	89.8	
Static bed height	15	3	86.8	4.2	77.0	55.7
Heating tube		4	90.5	5.6	57.7	
location	2	5	90.5	4.3	75.2	
Mass flow rate	817	6	93.2	5.4	59.9	2.70
Average air inlet		7	111.3	22.8	14.2	
temperature	81.6	8	142.2	35.6	9.08	
Heat flux	323.2	9	174.2	49.1	6.58	1.10
		10	187.2	97.2	3.33	
		11	203.0	110.0	2.94	

		Probe position	Tube wall temperature	Temperature difference	Local heat transfer coefficient	Bed density
Run Number	AC-19	1	86.3	8.5	37.7	
Type of beads	Fine	2	93.2	14.8	21.7	
Static bed height	3	3	95.3	15.3	20.9	5.90
Heating tube		4	99.0	18.3	17.5	
location	3	5	102.8	20.2	15.9	
Mass flow rate	1140	6	103.8	20.1	15.9	4.80
Average air inlet		7	105.3	20.6	15.6	
temperature	79.0	8	106.7	21.1	15.2	
Heat flux	320.5	9	107.8	21.5	14.9	4.40
		10	100.8	13.3	24.1	
		11	114.7	27.2	11.8	
Run Number	AC-20	1	89.5	5.6	57.0	
Type of beads	Fine	2	88.7	4.2	76.0	
Static bed height	3	3	94.7	9.8	32.6	3.60
Heating tube		4	105.2	19.9	16.0	
location	3	5	113.8	27.2	11.7	
Mass flow rate	817	6	121.7	34.0	9.38	1.10
Average air inlet		7	131.7	43.1	7.40	
temperature	82.5	8	138.2	48.3	6.60	
Heat flux	319.0	9	141.2	50.9	6.27	0.94
		10	134.7	42.8	7.45	
		11	159.5	68.9	4.63	
Run Number	AC-21	1	87.0	6.2	50.5	
Type of beads	Fine	2	86.5	5.4	58.0	
Static bed height	6	3	90.2	8.9	35.2	15.4
Heating tube		4	94.2	12.4	25.3	
location	3	5	99.2	16.2	19.3	
Mass flow rate	1110	6	101.3	17.1	18.3	6.60
Average air inlet		7	103.8	18.3	17.1	
temperature	80.6	8	105.5	19.1	16.4	
Heat flux	313.1	9	107.3	19.4	16.1	5.50
		10	100.0	12.0	26.1	
		11	114.8	24.7	12.7	
Run Number	AC-22	1	87.2	7.5	42.7	
Type of beads	Fine	2	86.3	5.9	64.0	
Static bed height	6	3	85.8	3.3	97.0	14.7
Heating tube		4	92.5	9.2	34.8	
location	3	5	106.8	21.8	14.7	
Mass flow rate	817	6	119.7	33.7	9.49	1.40
Average air inlet		7	133.8	47.0	6.81	
temperature	80.3	8	145.3	57.4	5.58	
Heat flux	320.1	9	152.2	62.9	5.09	0.62
		10	147.3	57.6	5.56	
		11	171.0	81.8	3.91	

		Probe position	Tube wall temperature	Temperature difference	Local heat transfer coefficient	Bed density
Run Number	AC-23	1	88.0	7.1	44.1	
Type of beads	Fine	2	87.2	6.8	46.0	
Static bed height	9	3	86.8	5.6	55.9	23.6
Heating tube		4	89.8	8.0	39.1	
location	3	5	92.3	10.3	30.4	
Mass flow rate	1155	6	97.2	14.1	22.2	8.60
Average air inlet		7	100.7	16.2	19.3	
temperature	79.4	8	103.3	17.2	18.2	
Heat flux	313.1	9	105.8	20.4	15.3	5.60
		10	98.3	12.8	24.5	
		11	113.3	27.9	11.2	
Run Number	AC-24	1	86.5	7.3	43.1	
Type of beads	Fine	2	86.2	6.6	47.7	
Static bed height	9	3	85.8	5.8	54.3	34.6
Heating tube		4	86.0	4.9	64.2	
location	3	5	91.2	8.7	36.2	
Mass flow rate	817	6	107.0	22.7	13.9	3.0
Average air inlet		7	125.2	39.8	7.91	
temperature	78.6	8	138.2	51.0	6.17	
Heat flux	314.9	9	145.8	58.2	5.41	0.60
		10	140.5	51.6	6.10	
		11	168.7	81.1	3.88	
Run Number	AC-25	1	78.7	5.7	55.8	
Type of beads	Fine	2	79.2	5.2	61.2	
Static bed height	15	3	79.8	4.9	64.9	47.9
Heating tube		4	81.3	4.9	64.9	
location	3	5	82.8	4.9	64.9	
Mass flow rate	1112	6	86.7	7.0	45.4	25.6
Average air inlet		7	90.0	9.7	32.8	
temperature	74.3	8	95.7	14.4	22.1	
Heat flux	318.0	9	99.8	18.7	17.0	9.00
		10	95.8	13.5	23.6	
		11	114.7	33.0	9.64	
Run Number	AC-26	1	88.0	8.4	37.4	
Type of beads	Fine	2	86.5	7.1	44.3	
Static bed height	15	3	86.0	5.7	55.1	50.5
Heating tube		4	86.0	4.5	69.8	
location	3	5	86.8	4.4	71.4	
Mass flow rate	817	6	89.2	5.4	58.2	30.6
Average air rate		7	96.5	11.4	27.6	
temperature	78.5	8	109.3	22.9	13.7	
Heat flux	314.2	9	123.7	35.8	8.78	2.50
		10	121.7	33.7	9.32	
		11	155.3	69.0	4.58	

Appendix Table 2

Type of beads *	Static bed height	Mass flow rate	Bed density, dense section	Bed density, sparse section	$h_{av.}$, dense section	$h_{av.}$, sparse section	$h_{av.}$, entire bed	hA	P	horsepower
F	3	828	4.05	1.35	29.9	9.17	16.5	225.7	8.09	.0055
F	3	1130	5.30	3.91	20.3	15.0	16.3	223.0	15.72	.0146
F	6	817	18.7	1.37	42.9	10.3	22.1	302.3	25.68	.0172
F	6	1143	14.2	6.05	33.8	17.0	22.5	307.8	33.90	.0319
F	9	736	33.8	1.77	57.4	11.1	28.0	383.0	44.73	.0271
F	9	1146	23.1	6.93	39.5	21.0	27.0	369.4	44.27	.0417
F	15	817	53.2	14.5	65.1	28.6	41.0	560.9	98.47	.0661
F	15	1120	44.9	18.0	48.9	29.3	35.3	482.9	96.91	.0892
C	3	2248	3.80	0.49	12.5	2.65	6.22	85.09	5.61	.0104
C	3	2800	5.58	1.30	11.7	4.23	6.18	84.54	9.80	.0226
C	9	1576	26.9	2.14	22.4	3.65	10.5	143.6	37.35	.0483
C	9	2269	25.7	3.03	23.0	8.02	13.3	181.9	38.05	.0713
C	9	2548	24.0	5.07	20.8	7.58	12.2	166.9	37.30	.0780
C	15	848	54.3	4.71	25.1	7.20	13.6	186.0	76.33	.0532
C	15	1449	50.6	8.35	23.0	8.25	13.4	183.3	80.62	.0960
C	15	2003	47.7	9.40	27.2	12.1	17.2	235.3	79.66	.1311
U		760					2.43	33.24	.017	.000011
U		818					2.47	33.79	.0184	.0000124
U		1140					2.72	37.21	.034	.000032
U		1480					3.01	41.18	.057	.000072
U		1980					3.41	46.65	.095	.000155
U		2480					3.84	52.53	.135	.000275
U		3200					4.43	60.60	.212	.000559
U		3960					4.93	67.44	.304	.000989
B		800					7.26	99.32	5.93	.0039
B		1135					8.85	121.07	11.35	.0106

* F Fine
C Coarse
U No beads, unbaffled exchanger
B No beads, baffled exchanger

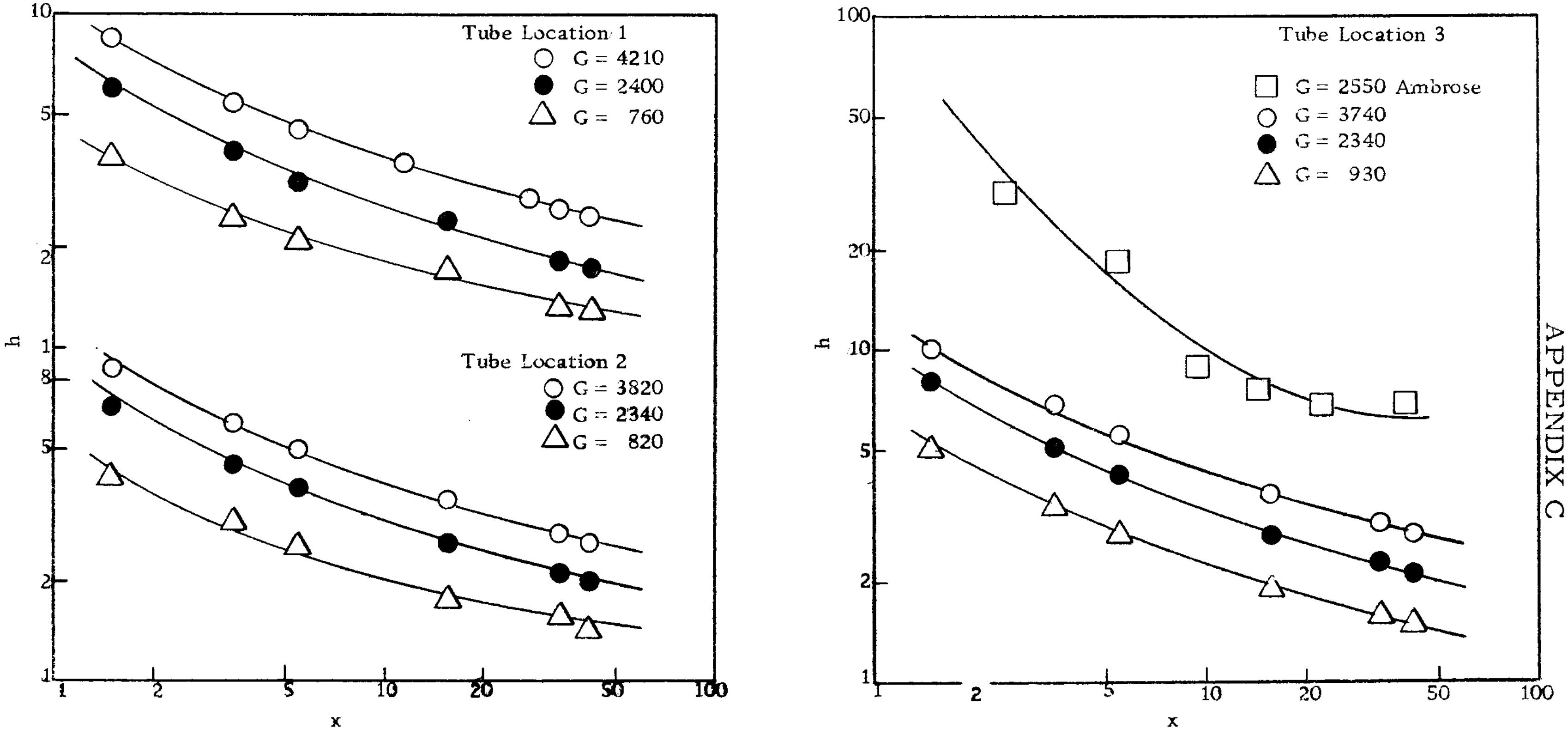

Figure 19. Local Heat Transfer Coefficient for Air

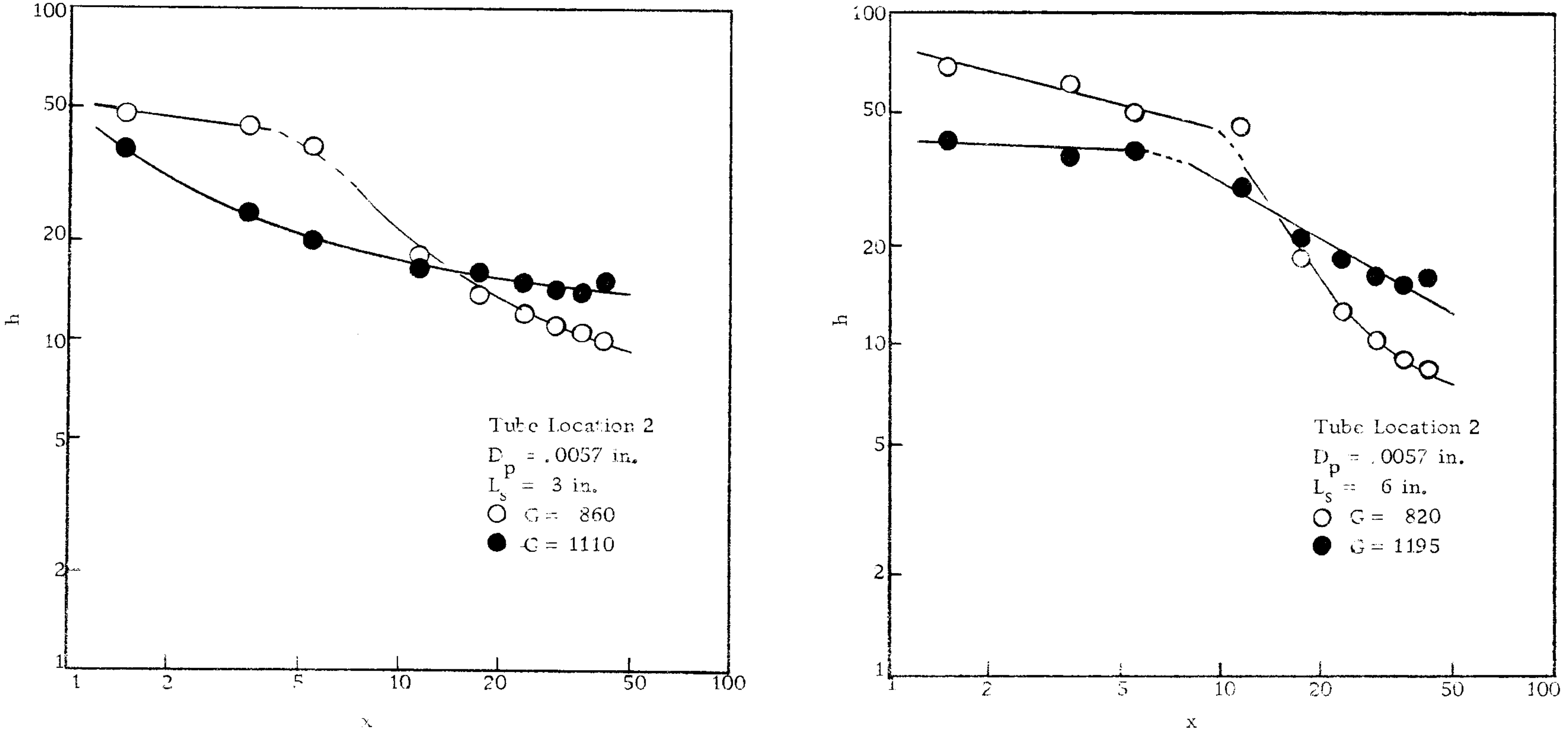

Figure 20. Local Heat Transfer Coefficient

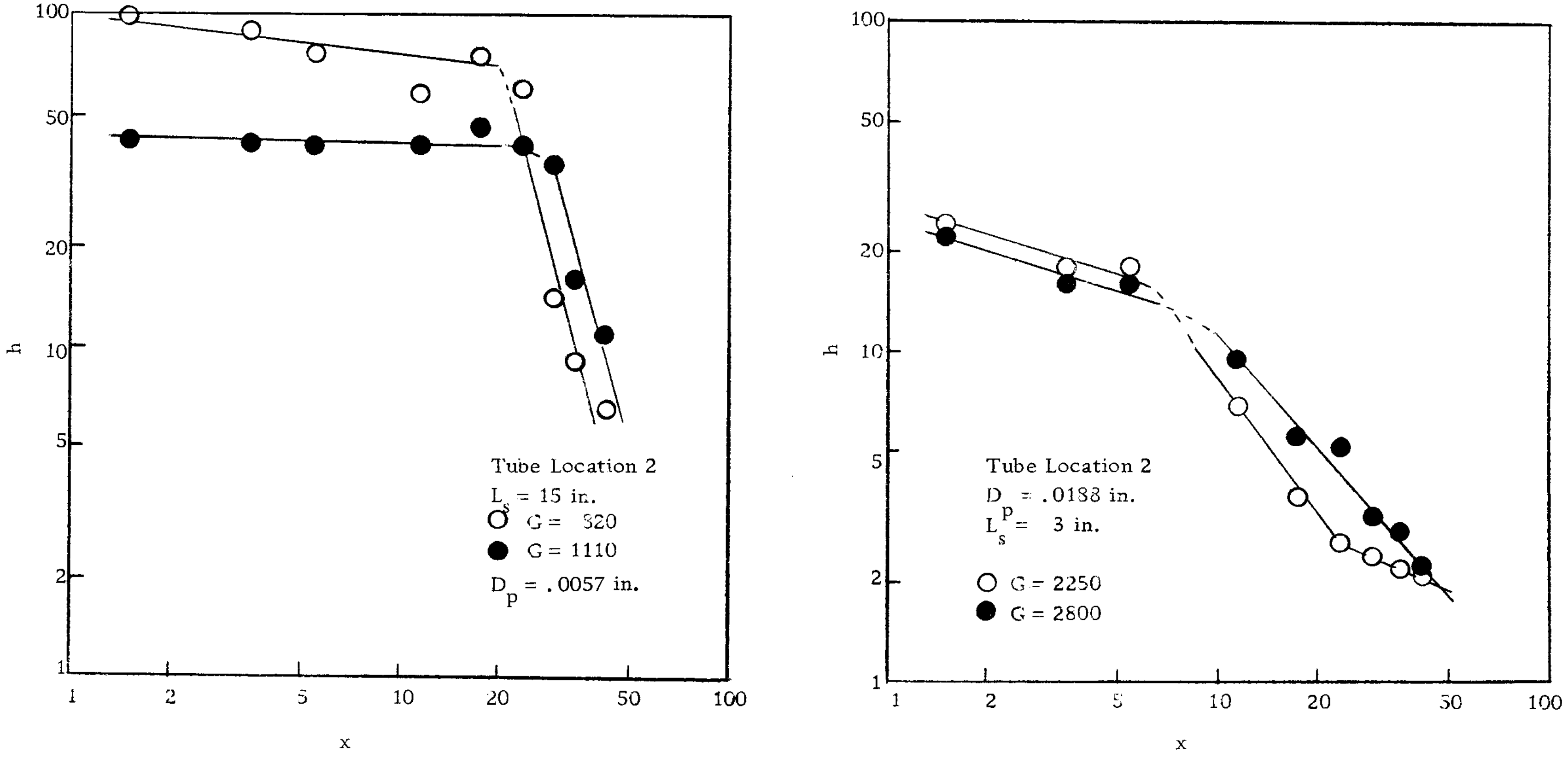

Figure 21. Local Heat Transfer Coefficient

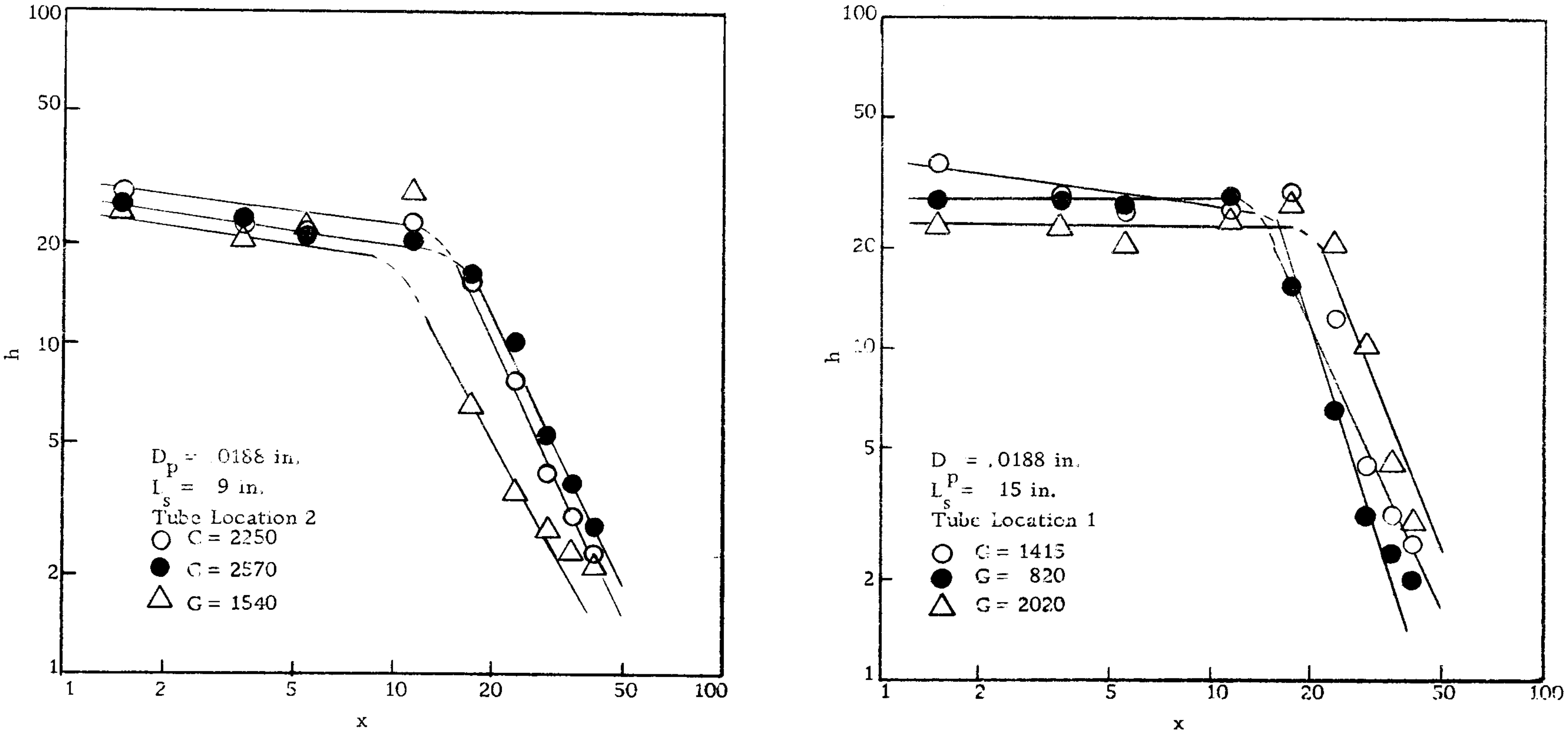

Figure 22. Local Heat Transfer Coefficient